KCFP

Annual Report

2017

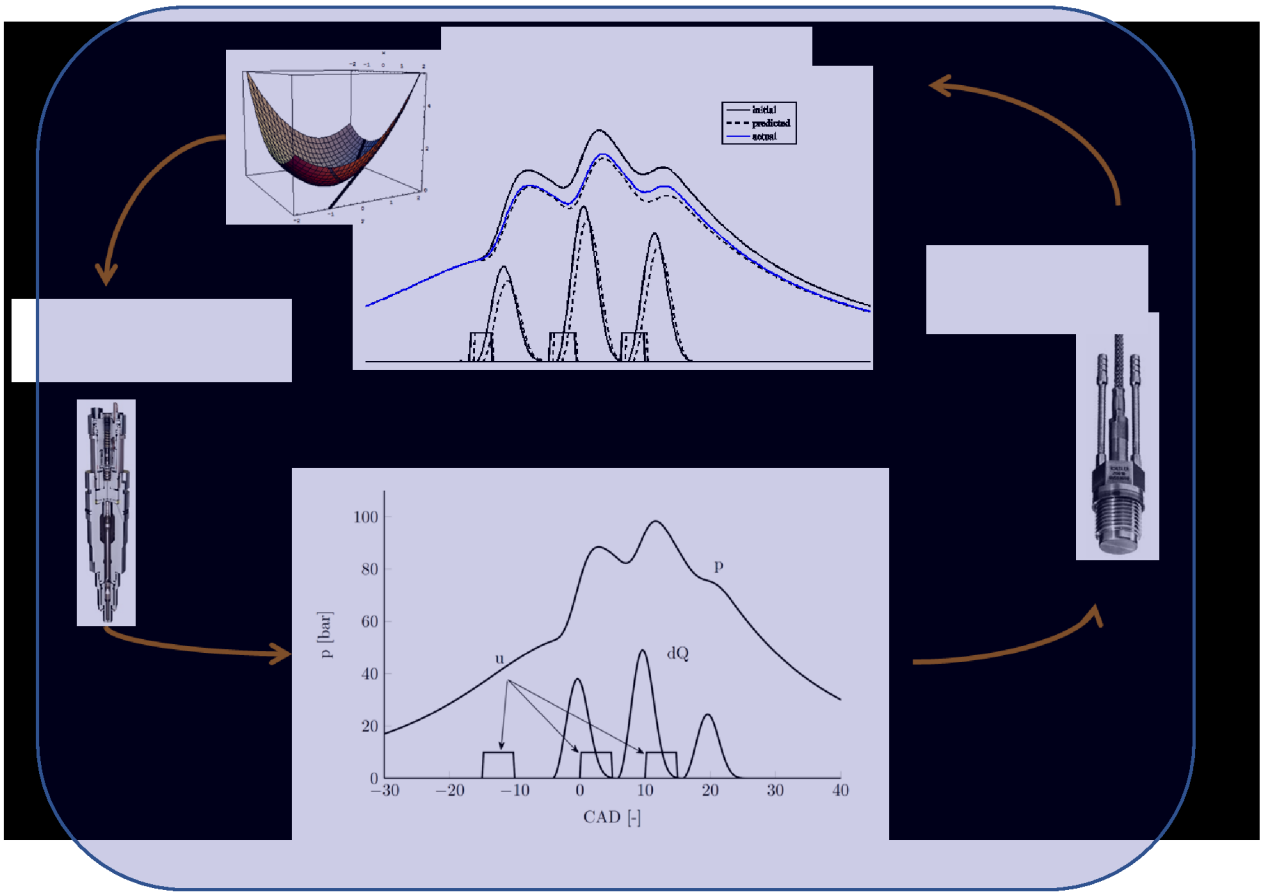

KCFP
Engine Research Center

LUND UNIVERSITY

Table of contents

The KCFP Engine Research Center

The KCFP Engine Research Center started July 1, 1995. The main goal of the center is to improve our understanding of the combustion process in internal combustion engines. Combustion processes with low enough temperature to suppress the formation of NOx and particulate matter are particularly interesting.

The center has a budget of 25.4 MSEK per year. The Swedish Energy Agency, Lund University and the Industrial member companies contribute roughly one third each to this budget.

KCFP Members

Lund University

The Swedish Energy Agency

Scania CV AB

Volvo Car Corporation AB

AB Volvo

Borg Warner Engine Group

Chevron Energy Technology Company

Cummins Inc.

Dantec Dynamics A/S

Loge

Swedish Biomimetics 3000 AB

Toyota Motor Corporation

Wärtsilä Finland Oy

KCFP Organization

BOARD

Sören Udd, Chairman
Johan Wallesten, AB Volvo
Annika Kristoffersson, Volvo Car Corporation AB
Per Stålhammar, Scania CV AB
Annika Mårtensson, Lund University
Sara Lönn, Lund University
Anders Johansson, Swedish Energy Agency

DIRECTOR
Professor
Per Tunestål
Supervisor
for: PPC,
Gas Engine

Administrator
Catarina Lindén

Professor
Rolf Johansson
Supervisor for:
PPC Control

Professor
Marcus Aldén
Supervisor
for: PPC and
GenDies

A. Professor
Martin Tunér
Supervisor
for: PPC

Professor
Öivind Andersson
Supervisor for:
GenDies GenDies

Professor
Mattias Richter
Supervisor for:
PPC and
GenDies

Professor
Xue-Song Bai
Supervisor
for: PPC

Partially Premixed Combustion (PPC) Project

The PPC project investigates partially premixed combustion in heavy duty and light duty engines to understand how this type of combustion can be used to improve both efficiency and emissions. The PPC project is composed of five subprojects:

- PPC – Heavy Duty: Thermodynamic engine experiments in heavy duty engines
- PPC – Light Duty: Thermodynamic engine experiments in light duty engines
- PPC – Modelling: CFD studies coupled with detailed chemistry
- PPC – Optics: Optical studies
- PPC – Control: Study of control challenges and opportunities

PPC – Heavy Duty

Introduction

Partially premixed combustion (PPC) is an advanced combustion strategy which has been proposed to gain higher efficiency and lower emissions than conventional compression ignition, as well as more controllability compared to homogeneous charge compression ignition (HCCI). The fuel-air stratification level is the key factor achieving these results. In the previous stage, the effect of injection strategy (injection timing in this case) on the stratification formation was investigated by doing a start of injection timing sweep called “transition from HCCI to PPC”. Except for the injection strategy, fuel properties and injector-piston geometry design are another two common methods to manipulate the stratification level. In the current work, the effect of fuel properties and piston geometry on stratification formation process was investigated using the same engine setup and control strategy. It turned out that at the same injection timing, different fuels could have slightly diverse stratification condition due to their physical properties diversity. And an optimization of the piston bowl shape did show significant potential of improving the controllability of PPC combustion.

Experimental setup

The experiments were conducted on a single cylinder heavy-duty compression ignition engine, modified from a Scania D13 6-cylinder engine of which five cylinders are deactivated. Figure 1 is the schematic of the engine and accessory equipment. The engine specifications are listed in Table 1. The injection system is a production XPI common rail injection system. The number of injections, the injection timing/duration could be adjusted as desired. The emission meter was composed of an AVL i60 emission meter and an AVL 483 micro soot sensor.

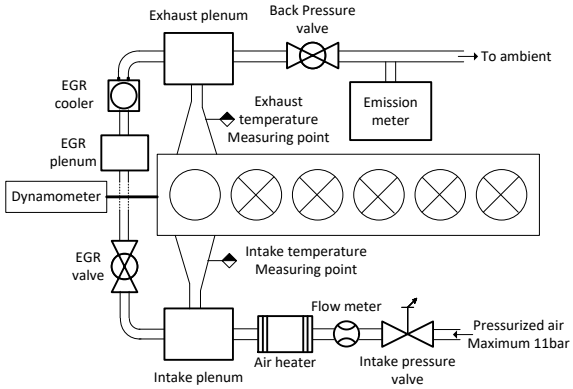

Figure 1: Schematic of the engine facilities.

Table 1: Engine specifications.

Displaced volume	2124 cc
Stroke	160 mm
Bore	130 mm
Connecting Rod	255 mm
Compression ratio	15:1
Swirl ratio	2.1
Exhaust Valve Open	43° BBDC
Inlet Valve Close	39° ABDC

Results

Effect of fuel properties on the stratification [1]

In this part, the effect of fuel properties on the fuel-air stratification formation was investigated. A PRF fuel was chosen to compare to the gasoline formerly tested. The properties of the fuels are shown in Table 2. The reason to use PRF81 instead of PRF87 is that, the PRF81 showed the same ignition delay as the gasoline when the SOI was at -27˚ATDC, with the same intake temperature. The required intake temperature of the PRF fuel comparing with the formerly tested gasoline was shown in Figure 2.

Table 2: Fuel properties.

Fuel type	Primary reference	Gasoline
RON	81	87
MON	81	81
H/C	2.279	1.92
O/C	0	0
Low Heating Value	44.46 MJ kg^{-1}	43.5 MJ kg^{-1}
Stoichiometric A/F	15.5	14.6
Vapor pressure	40.8 mmHg	232.6 mmHg
Heat of vaporization	0.317 kJ g^{-1}	0.38 - 0.5 kJ g^{-1}

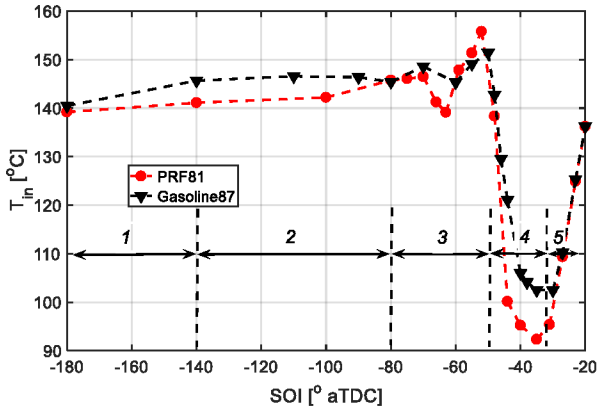

Figure 2: Required intake temperature comparison between PRF and gasoline.

It can be seen that the PRF and gasoline had different required intake temperatures at some SOIs but the overall trend matched. In zone 2, a slight increase in intake temperature was observed for both fuels. The intake temperature increment of PRF81 was 5°C lower than that of gasoline. In zone 2, the SOIs were early enough for both gasoline and PRF to form rather homogeneous mixtures. Both fuels could vaporize adequately. Thus, the difference of intake temperature should be due to the lower latent heat of PRF. In both zones 3 and 4, the temperature changes of the PRF with varying SOIs were always larger than those of the gasoline, no matter whether the temperature increased or decreased. In zone 3, only a small portion of the fuel spray was injected into the combustion chamber. The intake temperature difference is mainly because of the stratified level. The stratified level of PRF was always higher than that of the gasoline with the same injection timing since the volatility of PRF was lower than that of the gasoline. In zone 4, however, the whole fuel spray was injected into the combustion chamber. The lower latent heat of fuels also plays an important role in determining the required intake temperature. PRF had a lower latent heat thus it needed lower intake temperature.

Also considering the results of previous section, it could be concluded that in zones 1 and 2, the combustion was HCCI, while in zones 4 and 5 it was PPC. Zone 3 was a transition area, and its allocation being determined by the geometric design of the injector and the combustion chamber. This three-stage development of charge stratification exists universally in direct injection compression ignition engines, and the well-tuned distribution of these stages would be greatly beneficial in terms of engine efficiency and improved emissions. As previously mentioned, the piston used has a modified combustion chamber and the injector spray angle is 120˚, which is narrower than that of the production prototype. The stratification status as a function of the injection timing will differ if another piston–injector pair with different geometric parameters is used. Different settings could be beneficial for different combustion strategies. For example, if the spray angle was even smaller, the transition stage (zone 3) might be further reduced and the PPC stage (zones 4 and 5) would start earlier. If the intake temperature in zone 4 could fall more slowly, it would be very preferred for PPC, as it would give more flexibility and accuracy in controlling combustion phasing. Besides, less fuel would be trapped inside the crevice and the combustion efficiency could be improved.

Effect of piston geometries on the stratification

After investigating the effect of SOI and fuel properties on the stratification formation process, the effect of piston geometry was investigated. The piston used in the research of SOI effect was a modified straight-wall piston. In this section, the standard production piston was tested. The piston bowl shape of these two pistons are shown in Figure 3.

Figure 3: The piston bowl shape of two pistons. On the left is the modified straight wall piston. On the right is the standard production piston.

The differences of the two pistons are not only the bowl shape, but also the compression ratio. The straight wall piston has a compression ratio of 15 while the standard piston 17.3. The same experiment conditions as the straight wall piston test were applied when running the Cr 17.3 piston. Figure 4 shows the comparison of the required intake temperature of the two pistons.

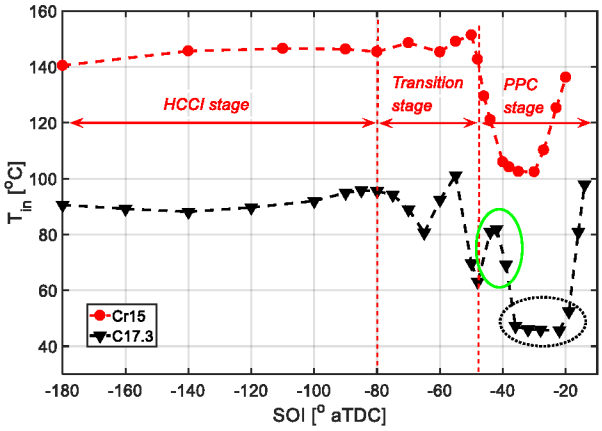

Figure 4: The required intake temperature of the two pistons.

The Cr17.3 piston needed roughly 50°C lower intake temperature than the Cr15 piston. The red lines mark the three stages of the Cr15 piston. For the Cr17.3 piston, these three stages also exist. But the allocation of them differ with the Cr15 piston, especially for the boundary of the transition stage and PPC stage. In previous

section, it is presumed that “if the spray angle were even smaller, the transition stage might be further reduced and the PPC stage would start earlier. The intake temperature in zone 4 (the early half of PPC stage) could fall more slowly, and this would be preferred for PPC, as it would give more flexibility and accuracy in controlling combustion phasing.” From this figure, this assumption was confirmed, although not by the way of using a smaller spray angle injector but a wider bowl piston. Inside the green ellipse is a quick increase and drop of the intake temperature. It is assumed to be caused by the complex profile of the combustion chamber. It needs further investigation by simulation or optical study. The simulation work is being done by the Division of Fluid Mechanics. Also, it would be more preferred if this unexpected increase and decrease of intake temperature doesn’t exist since it brought complexity to the combustion control. The black ellipse marks those operating points running at unchanged intake temperature. Due to the limitation of experiment setup, the intake temperature could not be lower than about 45˚C.

Conclusion

PPC is a novel diesel engine combustion strategy that could achieve high efficiency, low emissions over the whole engine load. The key advantage of PPC over the conventional diesel combustion and HCCI comes from the plentiful ϕ distribution inside the combustion chamber and which originates from the fuel-air stratification level. This project investigated several main influencing parameters of the stratification formation process, including the injection strategy (previous work), fuel properties and piston bowl geometries.

In the previous work, a start of injection sweep was conducted to investigate the change of stratification status during the transition from HCCI to PPC. Based on the different status of stratification, three stages, i.e., the HCCI, transition, and PPC stages were identified. This three-stage development of charge stratification exists universally in direct injection compression ignition (DICI) engines, and properly optimizing the allocations of these stages could have enormous benefits in terms of improving engine efficiency and reducing emissions.

In the current work, the effect of fuel properties on stratification formation was investigated. PRF81 was used to compare with the previously tested gasoline. PRF81 was believed having the same chemical properties with the gasoline in PPC conditions. The results showed that the PRF had the same character in terms of “five zones” and “three stages”. The differences were that at each stage, the required intake temperature of PRF slightly differed with that of gasoline. These differences were attributed to the physical properties of the fuels, e.g. higher vapor pressure and heat of vaporization of gasoline. It will be ideal to run another fuel which has the same physical properties with the previous tested gasoline but different chemical characters, to see the effect of chemical effects on the stratification formation process.

In the end, the effect of piston geometries on the stratification formation were investigated. The effects of two pistons with different chamber shape and compression ratio on the stratification formation were compared. Also this could be viewed as a verification of an assumption during the former research. That is, with some optimizations, e.g. using narrower spray angle injector or wider bowl mouth, can shorten the duration of the transition stage and result in longer PPC stage. This is especially beneficial to the controllability of PPC. The results did show that with this wider bowl piston, the early half of the PPC stage was extended about 50% more and the transition stage was reduced. However, an unexpected “bump” of the required intake temperature was observed within the PPC stage which was assumed to be caused by the real bump on the chamber wall.

Future Work

It is mentioned that it is more preferred if the unexpected increase and decrease of intake temperature inside the green ellipse of Figure 4 doesn’t exist. And a possible way to flat this “bump” is to remove the bump on the combustion chamber wall of the piston. Thus the idea is to build a piston model without the bump on the

chamber wall and the compression ratio same as the straight wall piston. Simulation work can be done with the new piston model and can compare the result with the experiment.

Papers Published

[1] Li, C., Tunestål, P., Tuner, M., and Johansson, B., "Comparison of Gasoline and Primary Reference Fuel in the Transition from HCCI to PPC," SAE Technical Paper 2017-01-2262, 2017.

PPC – HD Optics. High Load – High speed

Introduction

In this activity a Volvo MD13 engine was used, modified for optical access according to the Bowditch principle (Figure 5). This engine has been designed to cover the whole load range of the stock engine, including full load operation at 22bar $IMEP_g$. Detailed information on the optical engine can be found in [2]. The fuel used in these experiments was PRF87 and acetone was chosen as fluorescent tracer of the fuel (10% by volume).

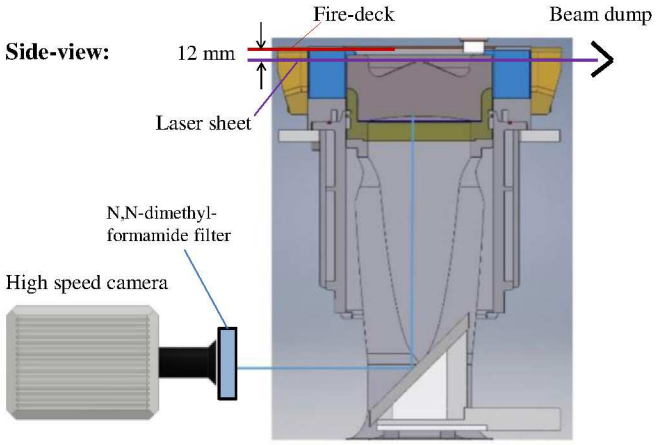

Figure 5: Experimental setup for the Volvo MD13 optical engine. The horizontal laser sheet is passing 12mm below the fire deck.

A state of the art, burst-mode laser system was used to provide a burst of 1000 pulses at a repetition rate of 36 KHz (Quasimodo, Spectral Energies). This repetition rate provided an outstanding temporal resolution of 5 frames per crank angle degree (CAD) (at 1200rpm), allowing for **cycle resolved** fluorescence measurements. A high speed camera was used to capture the images, running at twice the speed (72 KHz), allowing **on-line** (fluorescence) and **off-line** (chemiluminescence) measurements simultaneously.

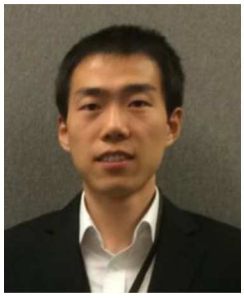

[redacted] [redacted] [redacted]

Cycle resolved - Planar Laser Induced Fluorescence

Fuel-tracer PLIF experimental setup

During the fuel tracer measurements, a wavelength of 266 nm laser light was used at 36 kHz, with a pulse energy of 50mJ. A laser sheet was formed by a cylindrical lens (f=-50 mm) and a spherical lens (f=+500 mm). The laser sheet was 65 mm wide, approximately equal to the width of the liner windows, and it was positioned 12 mm below the fire-deck (Figure 5). Acetone was used as the fluorescent tracer and 10% v/v was added in the fuel.

A high speed CMOS camera (Photron Fastcam SAZ) was used to capture the fluorescence signal with a 105mm Nikon objective lens (f#=1.8). The exposure time of the camera was set to 250 ns for mitigation of the high background luminosity during high load operation. The camera was running at 36 kHz with a resolution of 640x848, and at 72 kHz with a pixel resolution of 512x480. A long pass filter, which contains liquid N,N-dimethyl-formamide, was placed in front of the camera lens to avoid undesired scattered laser light.

CH_2O PLIF experimental setup

The 355 nm output from the burst system was used to excite CH_2O and partially oxidized fuel. The available energy was 180 mJ per pulse and the beam was directed through the same set of optical components (lens position was adjusted accordingly) as for the fuel tracer PLIF. An f=85 mm Nikon (f#=1.4) objective lens was used for signal collection in combination with a long-pass (GG385) filter for suppression of scattered radiation. In these experiments the laser system was operated at 36 kHz whereas the camera was running at 72 kHz to enable quasi-simultaneous detection of chemiluminescence. The acquisition time was set to capture in excess of 150 consecutive images from the start of injection to a few CADs after the start of combustion (SOC) within a single engine cycle.

Fuel distribution and CH_2O distribution at the start of combustion

Figure 6 demonstrates that, at the onset of combustion, the majority of the fuel mixture (green arrow) was not located at the same position as the spray plumes during the injection event (marked by the yellow contour). A high amount of fuel was located in the recirculation zone where two adjacent sprays impinge and merge together before the SOC. Apparently, under operating conditions with prolonged ignition delays, the region where the fuel originates during the injection event (yellow contour in Figure 6 (b)), contains almost no fuel at start of combustion. While the fuel gathered in the recirculation zone, the areas along the original spray axis are leaned out after the end of injection. This behavior, here captured within a single cycle, most likely constitutes yet another proof of the entrainment wave following immediately after the end of injection, as first

described by Musculus *et al.* [1].

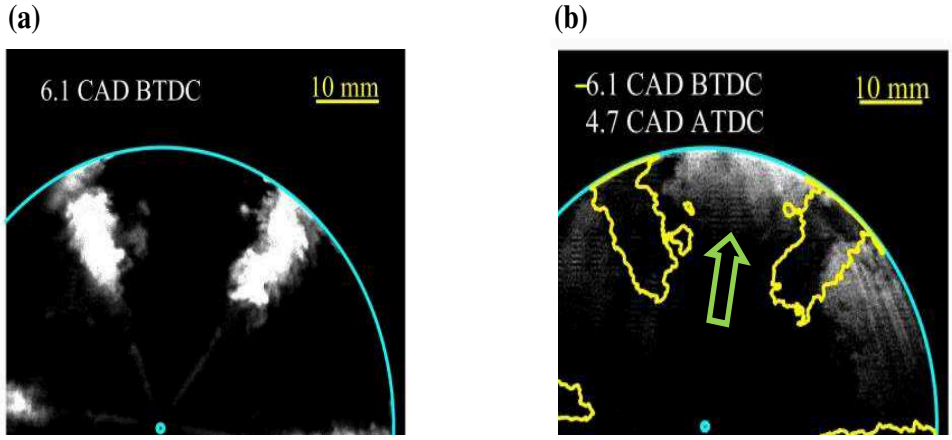

Figure 6: (a). Fuel distribution during the injection event at 6.1 CAD BTDC; (b). fuel distribution before SOC at 4.7 CAD ATDC together with the boundary layer of fuel distribution at 6.1 CAD BTDC (yellow lines).

Figure 7 shows the CH_2O distribution during the injection event and 0.1 CAD before SOC respectively. The green line represents the outer boundary of the CH_2O distribution at 6.1 CAD BTDC. As expected the CH_2O and fuel distributions follow a similar pattern, *i.e.* CH_2O also gathers in the recirculation zone where it was being pushed towards the center of the piston bowl before the SOC, while less CH_2O was located along the spray axis.

A unique feature of gasoline-like PPC is the long ignition delay, compared to diesel PPC. In the present study, CH_2O formation in the auto-ignition process wass found to persist until high temperature combustion starts consuming it, whereas the fuel (or rather fuel tracer) wass being decomposed slightly earlier.

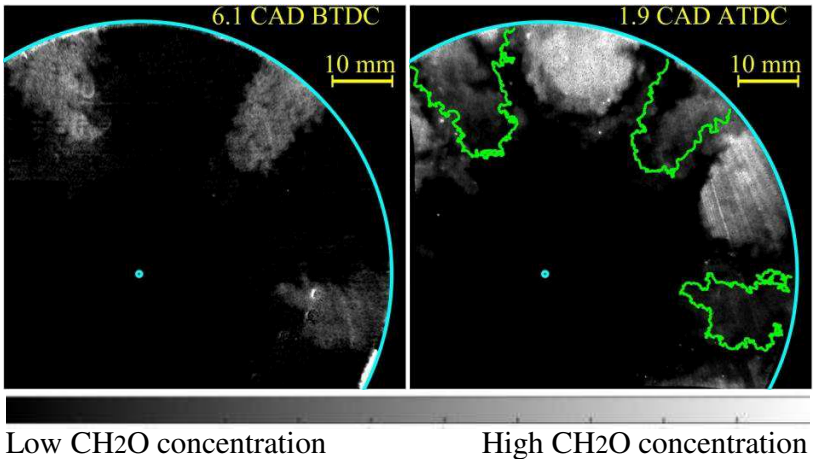

Figure 7: CH2O distribution before SOC at 1.9 CAD ATDC together with the outer boundary of CH2O distribution at 6.1 CAD BTDC (green lines) in one cycle.

Auto-ignition positions

In order to obtain the spatial relation between auto-ignition and fuel distribution, the outer boundary of simultaneously recorded chemiluminescence is imposed on the fuel PLIF images as shown in Figure 8. The red, green and yellow lines indicate the envelope of the flame at 0.3 CAD, 0.1 CAD before the recording of the fuel PLIF image and 0.1 CAD after it, respectively. The timing of the fuel PLIF image is indicated in the upper right corner of the image. Given the uncertainty of the line-of-sight integrated chemiluminescence, one can still see that the initial auto-ignition (left image in the upper row of Figure 8 was located close to the bowl rim in the center of the recirculation zone where most of the mixture resides after the ignition delay.

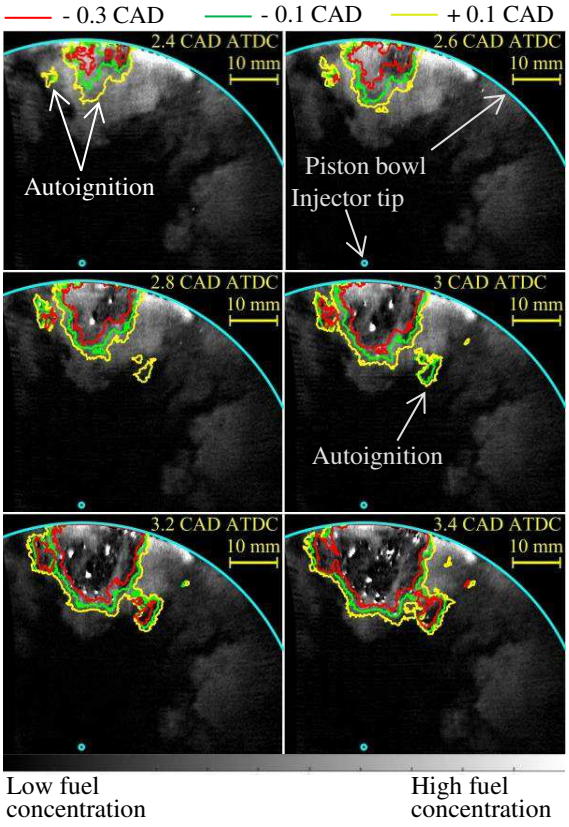

Figure 8: Fuel distribution after SOC together with envelope of auto-ignition zones. Red, green and yellow lines indicate flame luminosity at 0.3 CAD, 0.1 CAD before the PLIF image and 0.1 CAD after the PLIF image, respectively.

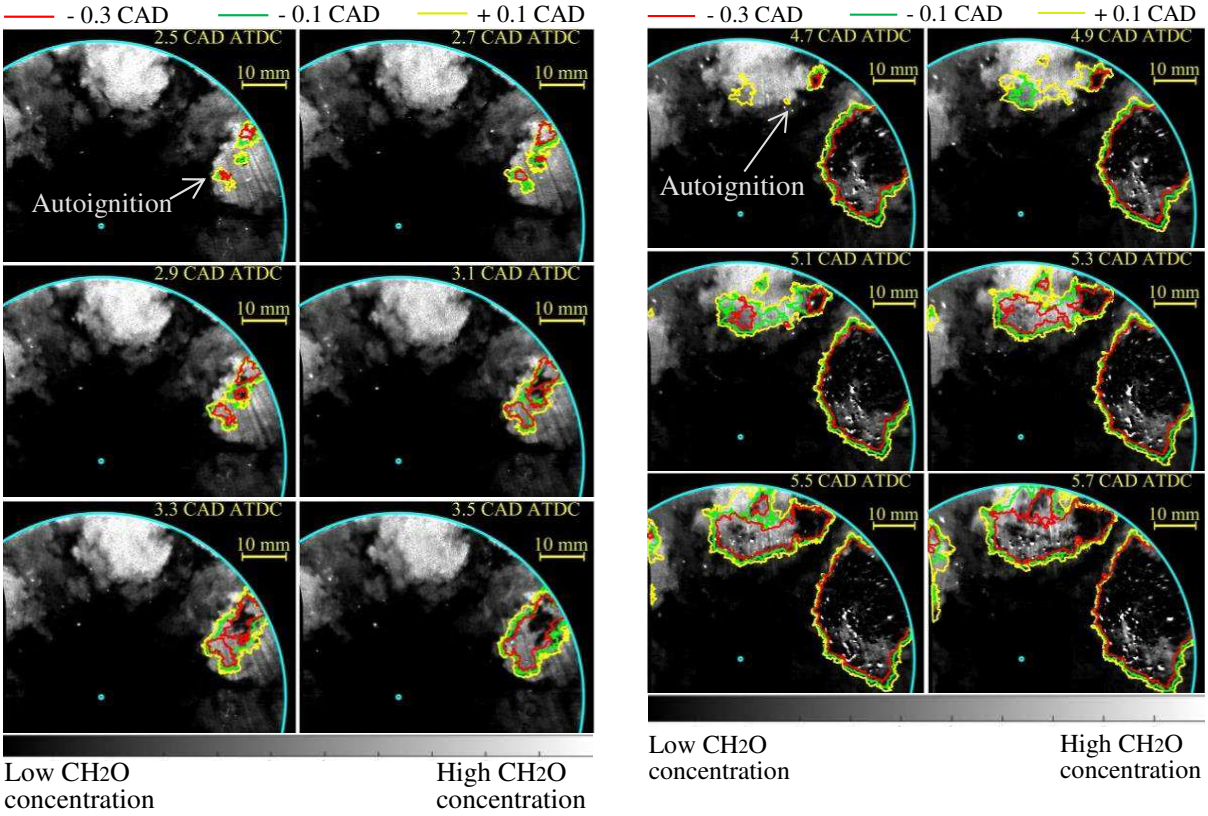

Figure 9: (Left) CH2O distribution after SOC together with envelop (curve notation, see Figure 8) of auto-ignition zones. (Right) CH_2O distribution during sequential auto-ignition events with envelop (curve notation, see Fig. 4) of the auto-ignition positions.

Similar to Fig. 4, the outer boundary of chemiluminescence is overlaid on the CH_2O PLIF image and presented in Figure 9, from 0.3 CAD ASOC to 3.7 CAD ASOC. The initial auto-ignition location (Figure 9 (left), top row) was found within the recirculation zone. The obvious difference between the chemiluminescence boundary and the 'holes' in CH_2O distribution in the recirculation zone (Figure 9 (left), bottom row) was a result of the PLIF images showing only two-dimensional cross-sections, whereas the chemiluminescence signal was line of sight integrated. Thus, the outer border from chemiluminescence represents the largest possible extent of the three-dimensional flame, as viewed by the camera.

In Figure 9 (right), the fuel located in the recirculation zones ignited first and the flame approached the outer boundary of the CH_2O distribution. The steep gradient of the charge causes the flame expansion rate to reduce significantly and finally come to a halt when there was no fresh charge to be consumed. The lack of combustible species and ignition precursors in the center of the combustion chamber became obvious. Additionally, in the same figure, the sequential auto-ignition of the upper recirculation zone can be studied. The consumption of CH2O in the upper recirculation zone, indicated by the growing holes in the CH2O distribution, was lagging the growth indicated by the chemiluminescence. This was a consequence of the 3D flame being initiated outside the plane imaged in the PLIF series. More detailed information can be found in KCFP Annual Report 2017.

High speed video investigations

High speed video measurements of chemiluminescence were also conducted in the same optical Volvo MD13 engine. The experiments were carried out at 1200 rpm with a constant load of 7 bar IMEPg, the fuel used was PRF87 and the intake oxygen level was kept at 16%. The high speed camera (Photron Fastcam SA-Z) was used to capture the combustion chemiluminescence with a resolution of 896 x 896 pixels, at a frame rate of 16 000 fps, resulting in 1 frame per 0.45 CAD (at 1200rpm). A short-pass filter (Ealing 35-5297-000 SP500nm cutoff) and a band-pass filter (UG11) were mounted in front of the camera to suppress soot radiation. The 135 mm Nikkor objective lens (F#=8) provided a 100 mm x 100 mm field of view (FOV). The camera was triggered at 5 CAD ATDC and its exposure time was set to 10 µs. 129 consecutive images were captured for each fired cycle.

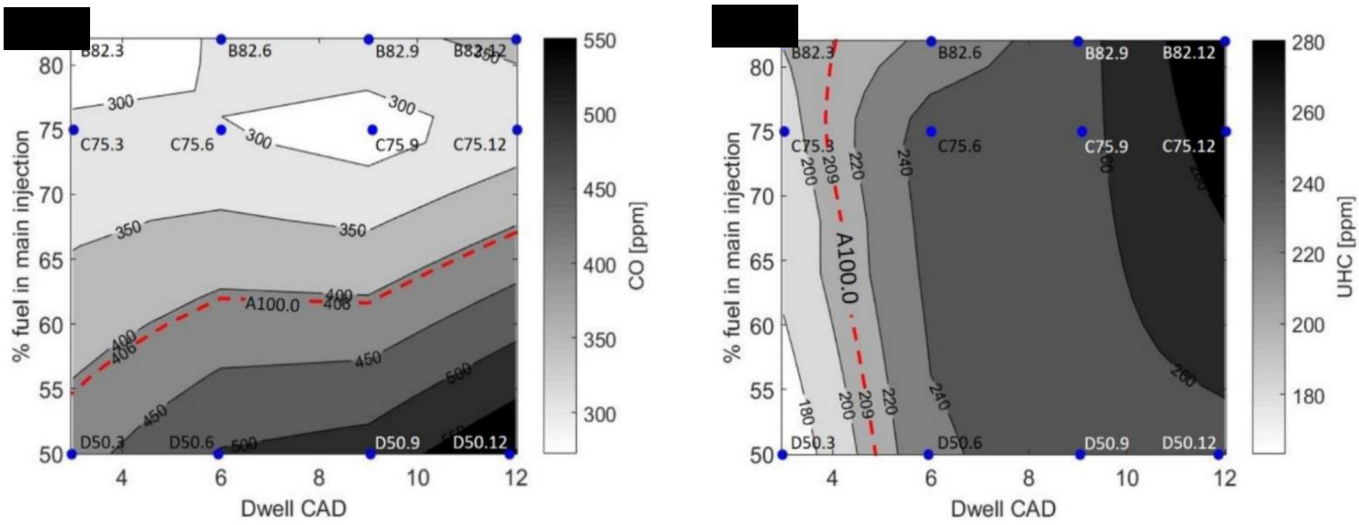

Figure 10: (a) CO as a function of injection ratio and dwell. The dashed red line marks the single injection emissions A100.0. (b) UHC as a function of injection ratio and dwell. The dashed red line marks the single injection emissions A100.0.

The CO and UHC emissions are shown in Figure 10 (a and b), where two general trends were observed. First trend showed the fuel ratio between main and post injections affects the CO emission, while the second trend indicated that the UHC were mostly affected by dwell time. Case B82.3, with a close coupled small post injection showed the best results, with reduction in both CO and UHC emissions compared to A100.0. However, separating the two, the close coupled large post injection D50.3 showed the biggest improvement in decreasing the UHC. More detailed information can be found in KCFP Annual Report 2016.

PPC – Light duty

Nikolaos Dimitrakopoulos - Lund University

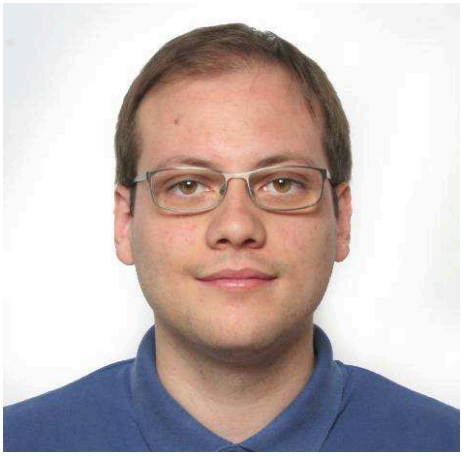

Giacomo Belgiorno – Istituto Motori CNR - Italy

Introduction

The PPC-LD (Partially Premixed Combustion – Light Duty) project focuses on the application of the PPC concept on a commercially available engine. PPC, an advancement over the older HCCI concept, promises both high fuel efficiency and low exhaust emissions, something that the traditional SI and CDC cannot provide at the same time. Low emissions are achieved by combining; high amount of EGR, around 30%-50%, to reduce the combustion temperatures and hence the NOx formation; and earlier injection timings, to premix the fuel and reduce the low oxygen areas that promote soot formation. High efficiency is due to the premixed type of combustion, a fast combustion event is possible, giving a higher effective expansion ratio.

During the last quarter of 2016 and the first quarter of 2017, the division of combustion engines co-operated with Istituto Motori CNR from Italy on the light duty PPC project.

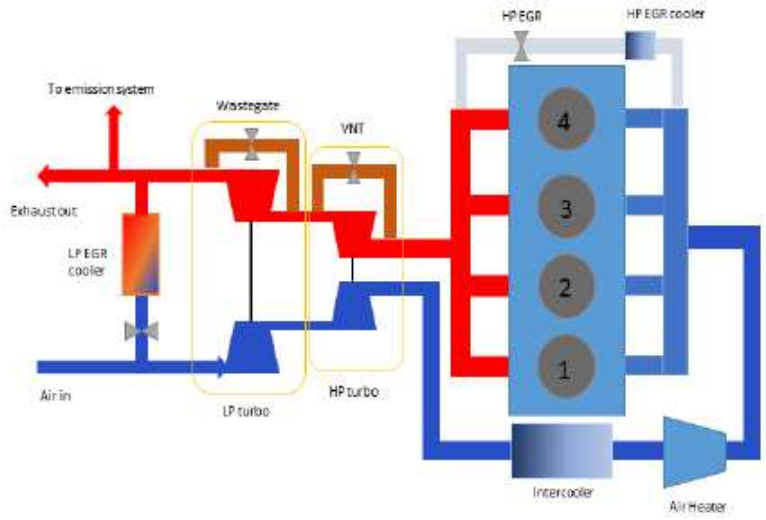

Figure 11 – Engine layout with the two different EGR routes

Parametric analysis effect of pilot quantity, combustion phasing and EGR on efficiencies of a Gasoline PPC light-duty engine.

A full factorial parameterization is performed in a 2 litre light duty engine (Figure 11) to evaluate the effects of rail pressure, EGR, combustion phasing and pilot quantity, under PPC conditions (Figure 12). These parameters were evaluated at three different RPM-load combinations, within the WLTC engine operating area. [1]

The DoE analysis shows high brake efficiency in PPC when adopting a high level of EGR (equal to 30%), low pilot ratio and advanced combustion phasing. Comparing this results with diesel combustion, the brake efficiency improves about 1.0% (at higher loads) at same NOx level and lower PM (two times). The improvement in efficiency can be attributed both to lower heat transfer losses due to high amount of EGR as well to faster combustion (Figure 13).

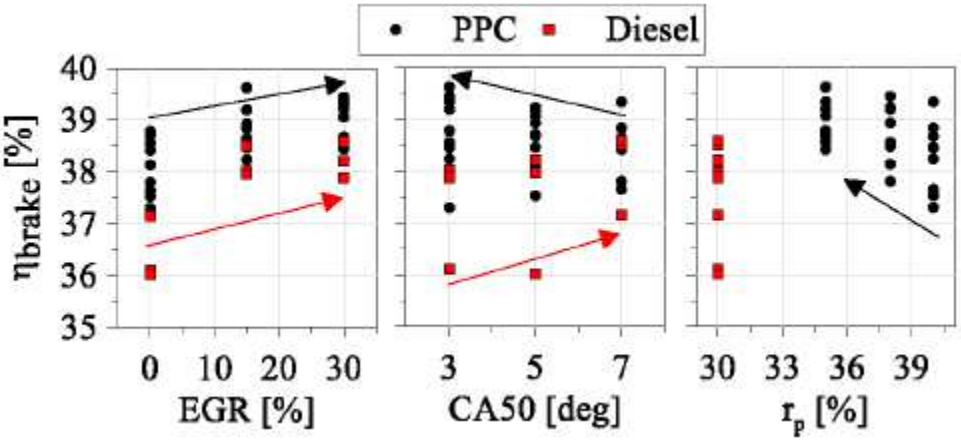

Figure 12 - Effects of EGR, CA50, pilot ratio on efficiency

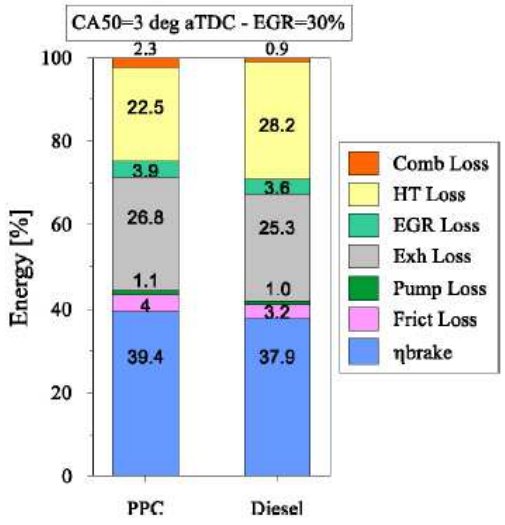

Figure 13 - Energy balance PPC and CDC

PPC operation with low RON gasoline fuel. A study on load range on a Euro 6 light duty diesel engine.

A commercially available diesel engine (2 litre Volvo Cars) is operated under PPC conditions from idle to maximum achievable full load with the use of low octane gasoline (RON 75) [2]. At low load the combustion stability is the limiting factor which leads to high COV (>5%) and high emissions in terms of carbon monoxide and unburned hydrocarbons. High load is limited by the maximum boost pressure and the necessary EGR rate which limit the available air. Through energy balance calculations heat transfer is reduced during PPC operation (Figure 14). With the use of a double injection strategy there is a benefit on the pressure rise rate while the fast combustion gives a high expansion ratio, leading to gross indicated efficiency of up to 50% (Figure 15).

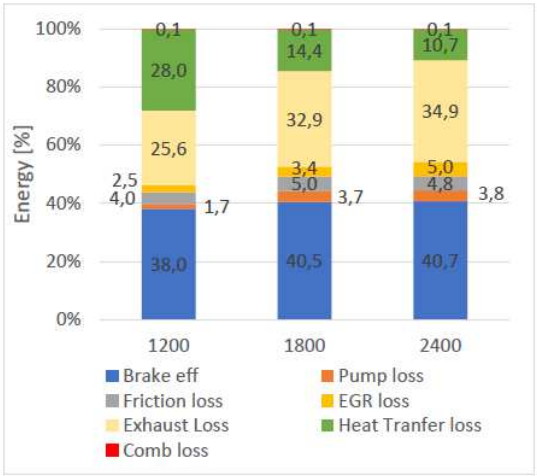

Figure 14: PPC energy balance at best efficiency.

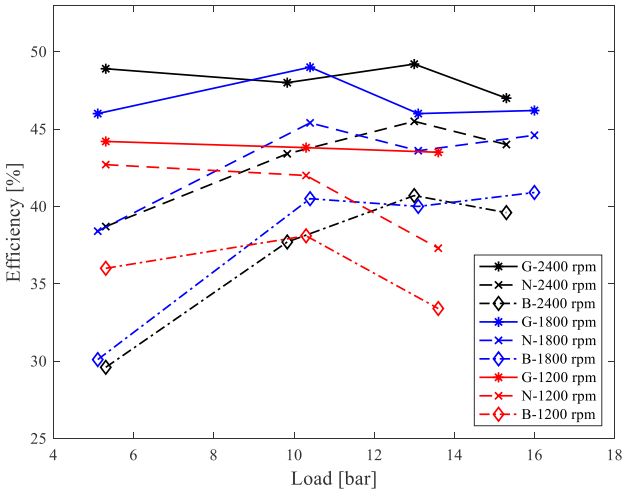

Figure 15: Gross (G), net (N) and brake (B) efficiencies.

Upcoming - Current Work

Effect of dual loop EGR on the efficiencies of a light duty PPC engine

While the use of EGR is the most common solution to reduce NOx emissions, the use of high pressure EGR (short route) has some drawbacks in terms of high gas temperature in the intake, soot contamination and a reduction of mass flow to the turbine. An alternative solution is the low pressure EGR (long route), where the exhaust gasses are drawn after the turbine and usually after the DPF. Research on diesel engines has shown some benefits of this approach and simulations under PPC conditions show benefits as well.

The next step is to evaluate the dual EGR route on the LD PPC engine, in terms of improving gas exchange efficiency, effect on diesel emissions (NOx, soot) and the possibility to expand to higher engine loads while maintaining adequate EGR levels.

Preliminary results show generally a positive effect in gas exchange efficiency (Figure 16) while maintaining the emissions at similar levels (Figure 17).

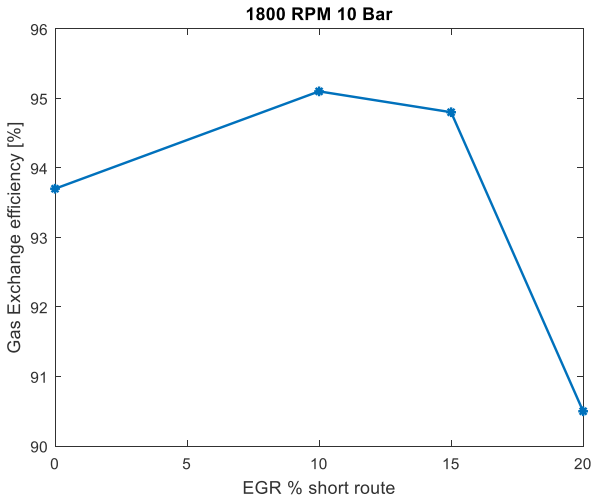

Figure 16: Effect of EGR split on gas exchange efficiency.

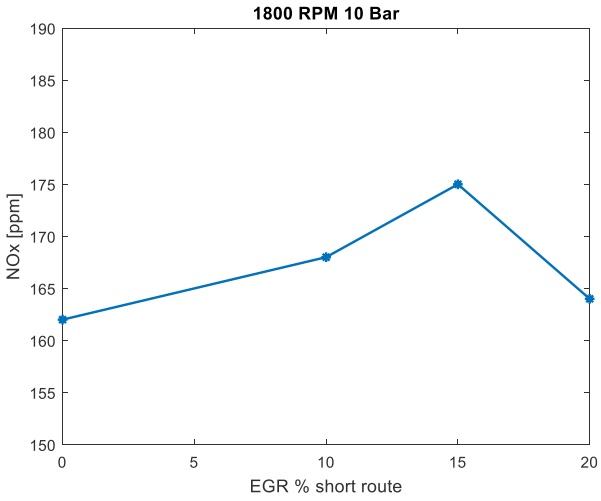

Figure 17: Effect of EGR split on NOx emissions.

References

[1] Belgiorno, G., Dimitrakopoulos, N., Di Blasio, G., Beatrice, C. et al., "Parametric Analysis of the Effect of Pilot Quantity, Combustion Phasing and EGR on Efficiencies of a Gasoline PPC Light-Duty Engine," SAE Technical Paper 2017-24-0084, 2017.

[2] Dimitrakopoulos, N., Belgiorno, G., Tuner, M., Tunestal, P., Di Blasio, G. & Beatrice, C. "PPC operation with low ron gasoline fuel. A study on load range on a euro 6 light duty diesel engine" COMODIA 2017 - 9th International Conference on Modeling and Diagnostics for Advanved Engine Systems. Japan Society of Mechanical Engineers

PPC – Modelling

Introduction

The goal of the PPC modelling sub-project is to improve the understanding of the PPC combustion process through 3D CFD simulations. The main focus of the simulations is on the fuel/oxidiser mixing in the cylinder and the effect of charge stratification on the combustion process and emission. This is intended to have a synergy along with metal engine experiments and optical measurements. While metal engine experiments yield definitive output values in terms of efficiencies and emissions and optical experiments provide measurements of physical quantities usually in two-dimensional physical space, certain physical quantities cannot be measured experimentally but they can be calculated using multiple dimensional CFD simulations. In a PPC engine context CFD simulation is particularly important since the fuel/oxidiser mixing is dominated by turbulent transport that is a three dimensional and unsteady phenomenon. The CFD tools used to model turbulent flow and combustion in the PPC engine modelling are dependent on the case which is studied, but since most simulations are calculated in engine-like geometries the most common way to model the flows is through the rather cost-effective Reynolds-average formulation of the Navier-Stokes equations (RANS). This means that the resulting modeled turbulence (and quantities transported by turbulence) will be an ensemble average of an infinite number of engine cycles. When studying small-scale flow details or cycle-to-cycle variations RANS model is insufficient and Large Eddy Simulation (LES) is utilised instead. The liquid droplets of fuel spray are studied using Lagrangian Particle Tracking (LPT) with suitable evaporation and breakup modelling. Because PPC ignition is sensitive to the chemical kinetics, fully coupling of the finite rate chemistry is needed. Methods of coupling the turbulence to the chemistry are investigated and used based on what is deemed necessary to answer the posed scientific questions. Typical methods include the well-stirred reactor model, partially stirred reactor model, stochastic fields and various flamelet based models.

Background and current focus

During past KCFP periods PPC combustion in diesel-type piston geometries has been investigated both in experimental work and in simulations. It has been shown that while PPC combustion can reach outstanding efficiencies and low emissions the combustion process is quite sensitive to parameters like cylinder gas temperature, fuel air mixing and wall temperatures. During the past year (2017) two CFD campaigns have been carried out to study the fuel/air mixing and combustion process in diesel like geometries. The first one is CFD study of the effect of the start-of-injection (SOI) on the mixing and combustion process in an optical engine (single injection, SOI -73 to -17 CAD ATDC, experiment performed in the KCFP PPC optical engine project). While the work covers model validation the focus has been on the analysis of the charge stratification and modes of combustion at different SOI. The second project is focused on a full cylinder simulation aiming at quantification of spatial and temporal development of the three-dimensional intake flow in different strokes of the piston motion and subsequently the effect of the large flow structures on the spray and fuel/air mixing.

Effect of SOI on the mixing and PPC combustion process

This work is based on the experiments carried out by Sara Lönn in an optical Scania D13 engine using PRF81 fuel. The experimental data shows the dependency of intake temperature to keep CA50 constant at 6 CAD ATDC for a single injection SOI sweep. Pictures of Mie scattering, and natural luminosity show spray penetration/impingement, the onset of first ignition sites in the cylinder, and the development of the reaction fronts. The aim of the project is to improve the understanding of the fundamental mixing and combustion process in the engine at different SOI. RANS k-epsilon model is chosen to model the flow and turbulence, and the spray is modeled using LPT considering both primary and secondary breakup of the spray. A 47-species chemical kinetic mechanism is used to model the combustion of PRF fuel. Because the ignition process is

sensitive to the finite rate chemistry, a direct coupling approach based on a well-stirred model (WSR) is used to integrate the chemistry with the turbulent flow calculations. The spray model breakup and penetration were calibrated using the Mie scattering data and the combustion phasing was adjusted by altering the intake temperature at IVC, in the same way as that in the experiments. Details of the results will be presented in a paper to be submitted for publication [1]. Some highlights of the results are given below.

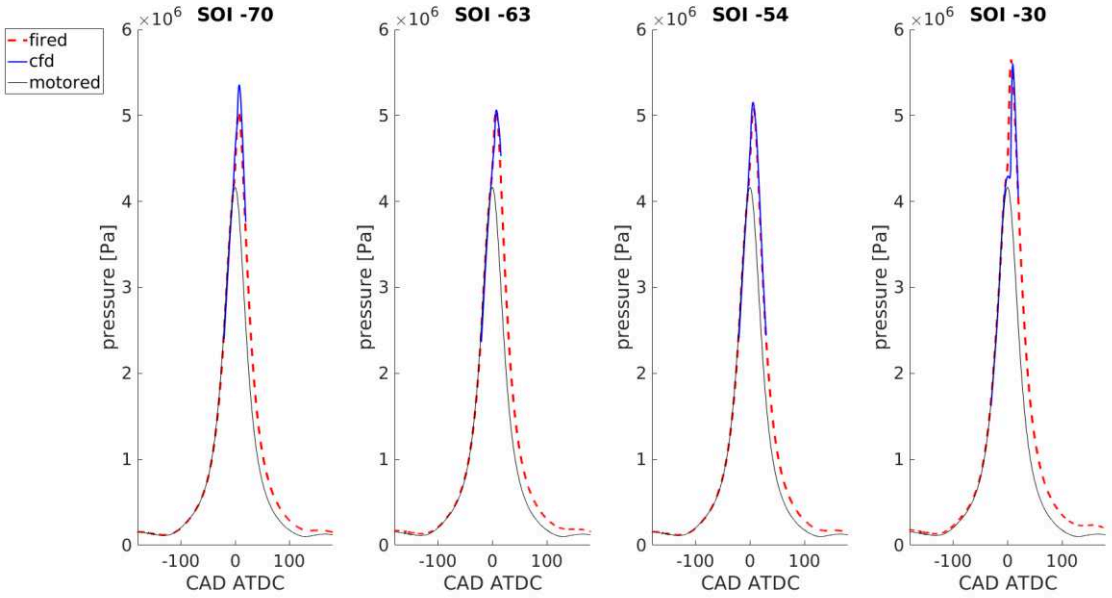

Figure 18. Pressure trace for various injection timings. As can be seen the WSR model captures the reaction rate rather well.

Figure 18 above shows the incylinder pressure trace at four different SOI. The experimental results under both motored run and combustion conditions (fired run) are compared with the CFD results obtained under combustion conditions. The CFD results under the motored run conditions are simulated as well and the results are identical to that of the experiments. For simplicity the CFD results under the motored run conditions are not shown in the figure. The experimental incylinder pressure is correctly replicated in the CFD when adjustment of the initial temperature of the mixture at IVC is made. Figure 19 shows the required intake temperature in the experiments to achieve a constant combustion phasing (with CA50 around 6 CAD ATDC) and the adjusted initial temperature in the CFD to achieve the same combustion phasing. With SOI earlier than -54 CAD ATDC the required initial temperature at IVC is rather similar to maintain the same combustion phasing, whereas further delay the SOI, e.g. to -30 CAD ATDC, the required initial temperature is much lower. This trend predicted in CFD is consistent with the experimental results. The difference between the intake temperature in the experiments and the initial temperature in CFD is likely due to the error in the wall temperature conditions used in the CFD as well as the error in the used mathematical models.

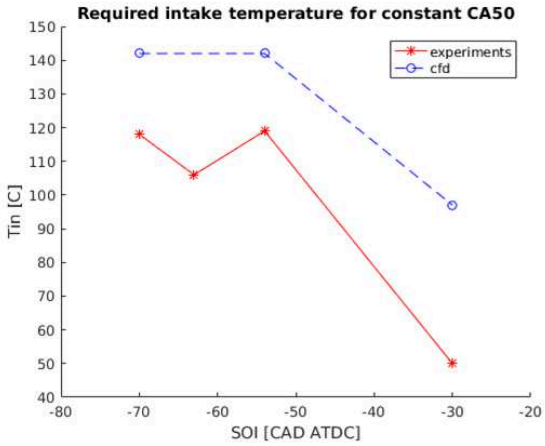

Figure 19. Required intake temperature in the experiments for a constant CA50 and adjusted initial temperature at IVC in the CFD simulations.

The CFD results reveal that for the early injection cases, e.g., SOI -70 CAD ATDC shown in Figure 20, the mixture at the onset of auto-ignition is more homogeneous. In the present engine operation, the equivalence ratio of the mixture in the bowl and the squish region is lower than 0.4. Ignition occurs at very low equivalence ratios (Phi ~ 0.3), which causes a slow combustion rate and lower combustion temperature, with a lower NOx formation rate. The lean mixture requires a higher intake temperature to ignite. With early injection (SOI earlier than -54 CAD ATDC) the mixture distribution in the bowl and the squish region are all fairly homogeneous. Thus, the charge stratification in these cases is similar and insensitive to the injection timing. This is the reason behind the nearly constant intake temperature required to achieve the same combustion phase in the different SOI cases with early fuel injection.

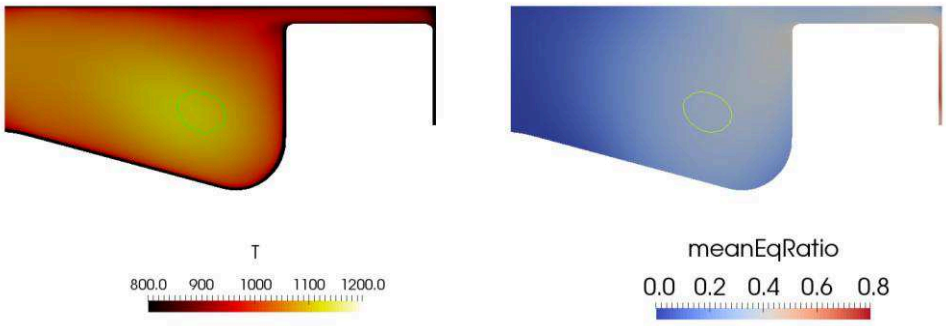

Figure 20. Ignition location for the SOI -70 CA case at 3 CA BTDC. The case ignites at an equivalence ratio [Phi] about 0.3. In-cylinder temperature at IVC is 420 K. The green ring is an iso-line for heat release rate typical during ignition.

With later injections, e.g. SOI -30 CAD ATDC as shown in Figure 21, the fuel/air mixing has short time before the onset of combustion; thus, the mixture is more stratified. The locally fuel richer mixture (Phi ~ 0.7) requires a lower intake temperature to achieve the same combustion phasing, which should increase the thermodynamic efficiency, but the heat loss is likely higher due to the higher combustion temperature and that combustion occurs close to the wall. The higher combustion temperature also gives rise to higher NOx formation.

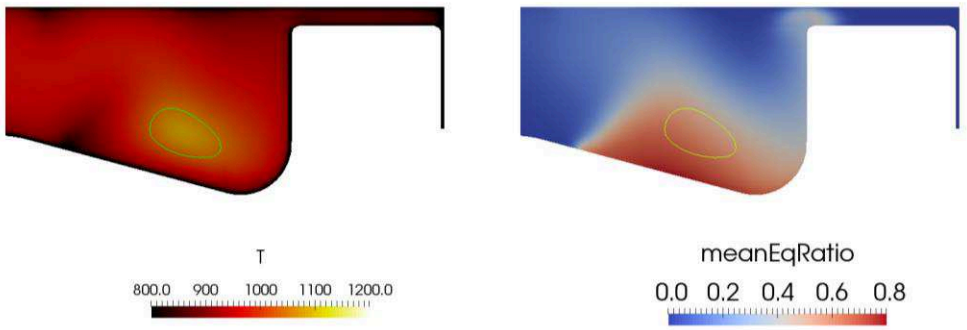

Figure 21. Ignition location for the SOI -30 CA case at 4 CA ATDC. The case ignites at an equivalence ratio [Phi] about 0.7. In-cylinder temperature at IVC is 376 K. The green ring is an iso-line for heat release rate during ignition.

CFD study of swirl and tumble flows in a light duty PPC engine

In PPC engines the combustion and ignition processes are sensitive to the mixing field. The mixing process is strongly affected by the incylinder flow and turbulence structures, as such the often-used assumption of the solid body rotational flow as the initial condition of compression stroke flow simulation may not be adequate. CFD simulation of the in-cylinder flow was performed with and without the consideration of the intake flow manifolds. The studied engine is a Volvo D5 light duty engine with a re-entrant piston bowl geometry. The aims were to quantify the evolution of the tumble and swirl motion in the cylinder in the intake stroke and the compression stroke, to discriminate the impact of the intake flow on the flow structures in the compression stroke, and to quantify the effect of the detailed swirl and tumble flow motion on the spray and fuel/air mixing process.

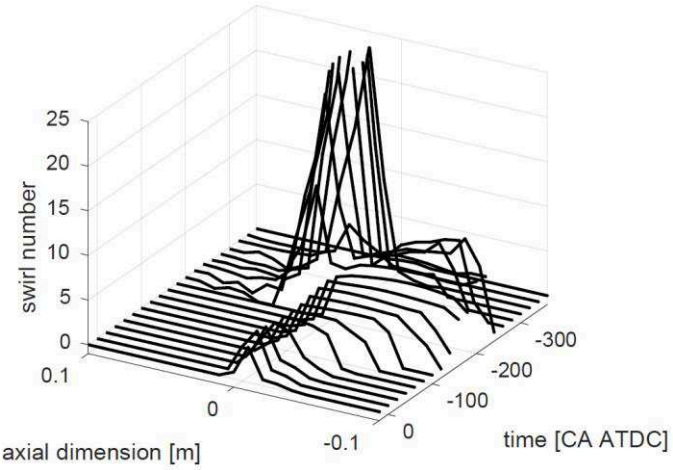

Figure 22. Planar swirl number at different axial position developing in time. Axial position 0 corresponds to cylinder head and positive scale corresponds to intake runner and manifold. New swirl sampling planes are introduced and removed as piston moves.

Figure 22 shows the swirl number defined at the cross-section plane in the intake manifolds and the cylinder. The axial distance z=0 is defined at the cylinder head, while z<0 is the intake manifolds and z>0 represents the cylinder. At the initial state (-360 CAD) the swirl number in the cylinder is 0.26, while in the intake manifolds the swirl number is zero (no flow motion). The local planar swirl number in the intake manifolds increases

rapidly to a value about 25 and maintained a much higher value throughout the intake stroke. As the intake flow approaches the valve opening the swirl number shows a decrease due to the sudden expansion of the intake flow into the cylinder; further downstream in the cylinder the swirl number increases until very close to the piston.

For the engine configuration studied in this work, the flow in the intake stroke is driven by two different mechanisms: (a) at the earlier intake stroke (from -360 CAD to -320 CAD ATDC) it is driven by the pressure difference between the intake and the cylinder, and (b) at later intake stroke (later than -320 CAD ATDC) the flow is driven by the piston motion. In the pressure driven stage the turbulent kinetic energy in the cylinder increases rapidly and then decays at the end of the pressure driven stroke. In the piston driven stage, the turbulent kinetic energy in the cylinder increases with the piston velocity and then decreases as the piston is decelerated at the end of the intake stroke. The intake flow manifolds result in the formation of the swirl motion in the intake, which subsequently induces the formation of the swirl flow motion in the cylinder. In the pressure driven flow stage a strong tumble flow motion is generated in the cylinder and in the piston driven stage the swirl flow motion in the cylinder is developed. The swirl number increases with the piston velocity and decreases as the piston is decelerated in the later intake stroke. In the intake stroke the rotational flow structure is complex: the axis of the rotation is deviated from that of cylinder axis, and center of the rotation is not on the center of the axis. This asymmetric flow structure is maintained throughout the entire intake stroke and remains significant in the intake stroke as later as -30 CAD ATDC. It is envisaged that with earlier injection PPC (e.g. SOI at -60 CFD ATDC) the asymmetric flow motion could affect the mixing field. In the compression stroke, the tumble flow motion is suppressed and as such the flow approaches to the structure of solid body rotational flow, with the rotation axis in alignment with the cylinder axis. The cylinder volume averaged turbulent kinetic energy and the swirl number from CFD with the full engine geometry are in general on good agreement with that from the sector mesh CFD that assumes axis-symmetric solid body rotational initial flow. It is expected that for diesel injection near TDC, the assumption of solid-body rotational initial flow and sector mesh could be adequate.

Details of the results are referred to the paper of Ibron et al. [2].

Papers and manuscripts

[1] C Ibron, M Jangi, XS Bai, Effect of SOI on the transition from HCCI to PPC in a heavy-duty diesel engine. Manuscript in preparation, 2018.

[2] C Ibron, M Jangi, T Lucchini, XS Bai, Numerical Estimation of Asymmetry of In-Cylinder Flow in a Light Duty Direct Injection Engine with Re-Entrant Piston Bowl, SAE Technical Paper 2017-01-2209, 2017.

PPC – Control

Fuel-Injection Control

Gabriel Turesson

Gabriel@control.lth.se

Predictive Pressure Control with Constraints

A predictive cylinder-pressure feedback controller that actuates fuel-injection amounts and timings with the objective of efficiently fulfilling constraints on peak pressure, pressure-rise rate, NO formation and exhaust temperature was developed. An in-cylinder-pressure tracking problem was also considered where the task is to follow a given pressure-reference trajectory. The controller employs the principle of model predictive control (MPC) where the fuel-injections is repeatedly optimized with respect to a receding time horizon of future engine cycles. Due to nonlinearity of the optimization problem, a quadratic-program (QP) approximation is performed each engine cycle through pressure-model linearization. A linearization method that was previously presented in [Ingesson et al., 2015]. The problem of separating the estimated heat-release rate in order to distinguish the contribution of different fuel injections was also studied. The controller was evaluated experimentally in the mid-load region of a Scania D13 heavy-duty engine, running on a gasoline fuel mixture.

Method

The controller principle is illustrated in Figure 23. The controller receives the previous-cycle in cylinder pressure signal every engine cycle. With the in-cylinder pressure signal, the heat-release rate is computed, and a pressure model is used to predict how the pressure varies with fuel-injection timing and injected fuel amount. NO emission were computed using the two-zone NO-formation model used in [Muric et al., 2014]. A first order model was used to model exhaust temperature dynamics as presented in [Eriksson et al., 2014]. The model-based prediction allows the controller to optimize the fuel-injection configuration for the next engine cycle. This procedure is then repeated every engine cycle and establishes a feedback loop.

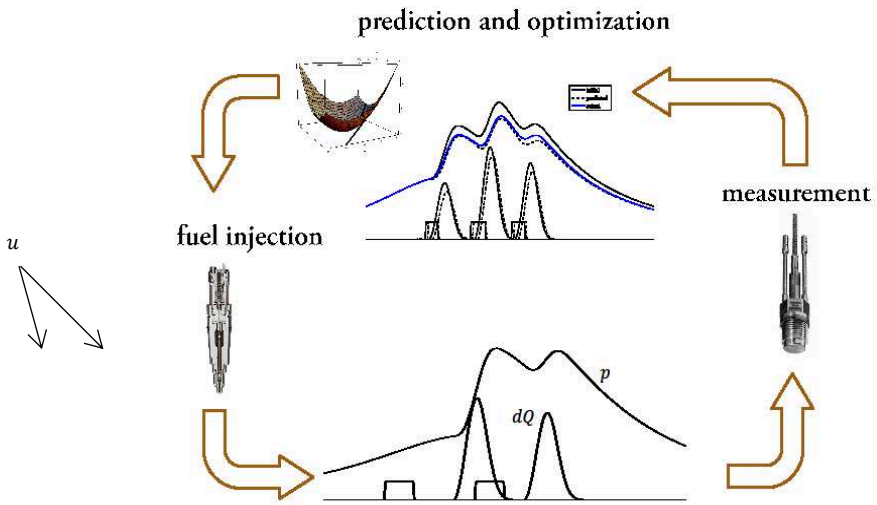

Figure 23. The controller solves the problem of deciding the injected fuel amounts and injection timings u which determines the current pulses sent to the fuel injector. $u = (\theta_{SOI}^1 \quad m_f^1 \quad \cdots \quad \theta_{SOI}^N \quad m_f^N)$

Two different optimal-control problems were considered.
The first optimization problem aims to fulfill constraints on peak pressure, pressure-rise rate, NO formation and exhaust temperature whilst penalizing fuel consumption, load-tracking error and control action. Fuel consumption was minimized by tracking an efficient combustion timing set point. This optimization problem was formulated according to

$$\begin{aligned} \underset{u}{\text{minimize}} \quad & \sum_{i=1}^{N_p} \text{fuel consumption}_i + \text{load tracking}_i + \text{control action}_i \\ \text{subject to} \quad & p \le c_{pmax} \\ & dp/d\theta \le c_{dpmax} \\ & NO \le c_{NO} \\ & T_{ex} \ge c_{T_{ex}} \\ & u \in U \end{aligned}$$

In addition, an optimization problem where deviation from a reference pressure curve was also considered. The pressure reference was here computed from an ideal limited-pressure cycle:

$$\begin{aligned} \underset{u}{\text{minimize}} \quad & \sum_{i=1}^{N_p} \text{pressure} - \text{tracking error}_i + \text{control action}_i \\ \text{subject to} \quad & u \in U \end{aligned}$$

The optimization problems above were solved with respect to a linearized cylinder-pressure model and feasible injection configurations U.

A combustion-detection method was developed in order to separate the influence from different injections, the method is summerized in Figure 24 for three injections. When the heat-release is separated it is possible to predict pressure changs with repsect to the different injections.

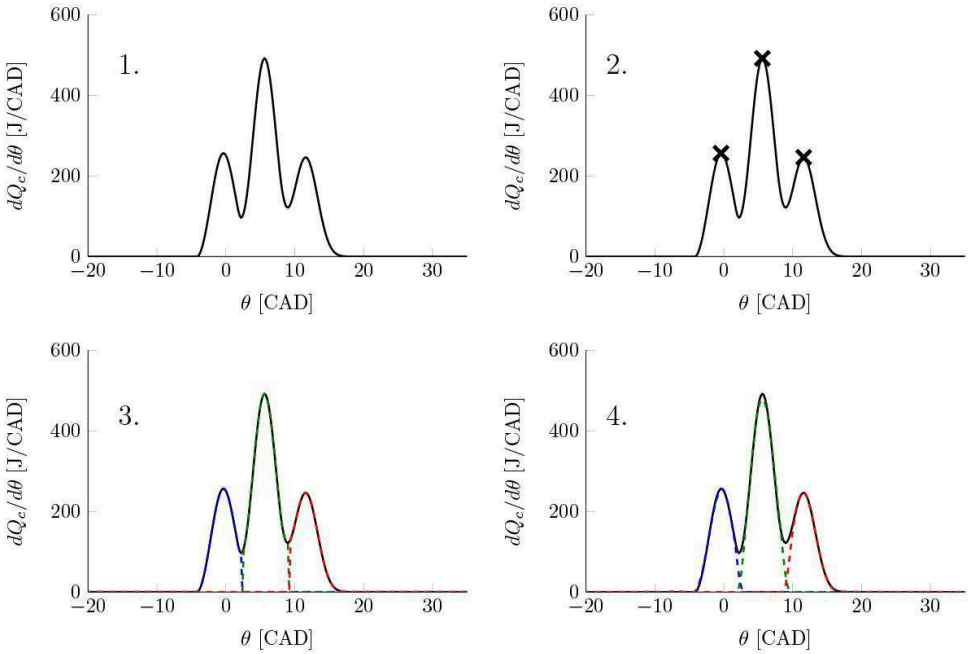

Figure 24 A method for separating $dQ_c/d\theta$ among the different injections (from 1 to 4). First the heat-release rate is obtained from the measured pressure signal (1).The most significant M peaks are detected (2), $dQ_c/d\theta$ is then separated in different intervals (3) according to the peak locations. The heat-release rates $dQ_c^j/d\theta$ are then filtered and normalized (4).

Experimental Evaluation

The controller with optimziation problem 1 above was evaluated by testing constraint fulfilment during transient engine operation. Maximum-pressure constraint fullfillment is presented in

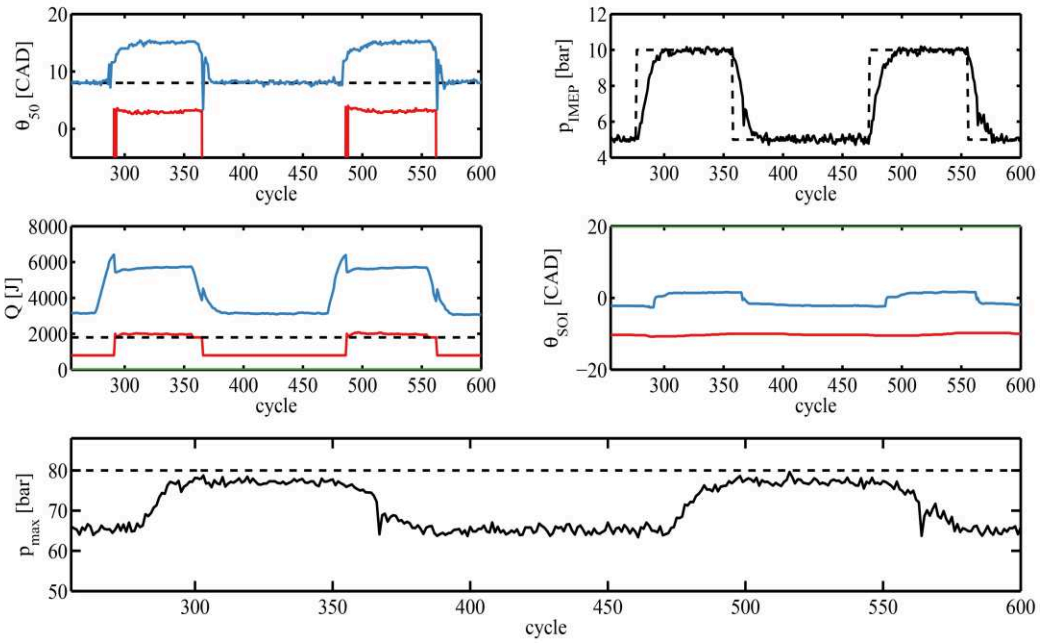

Figure 25, which displayes combustion timings (upper left), load (upper right), injected fue l energy (middle left), injection timing (middle right) and maximum pressure (lower). In-cycle data for cycle 45 (left) and 80 (right) are presented in

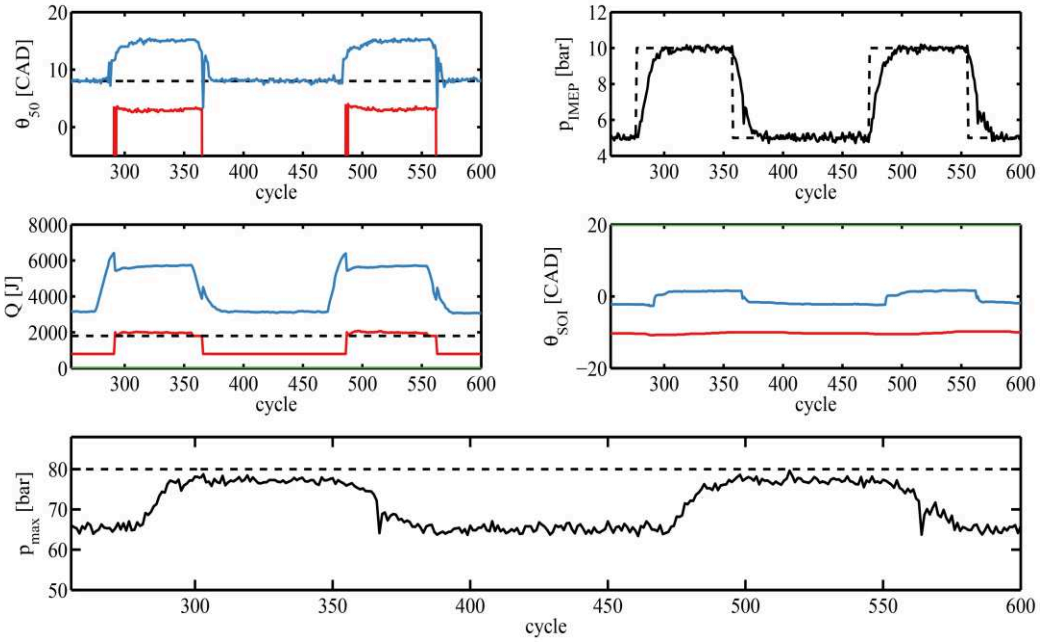

Figure 25

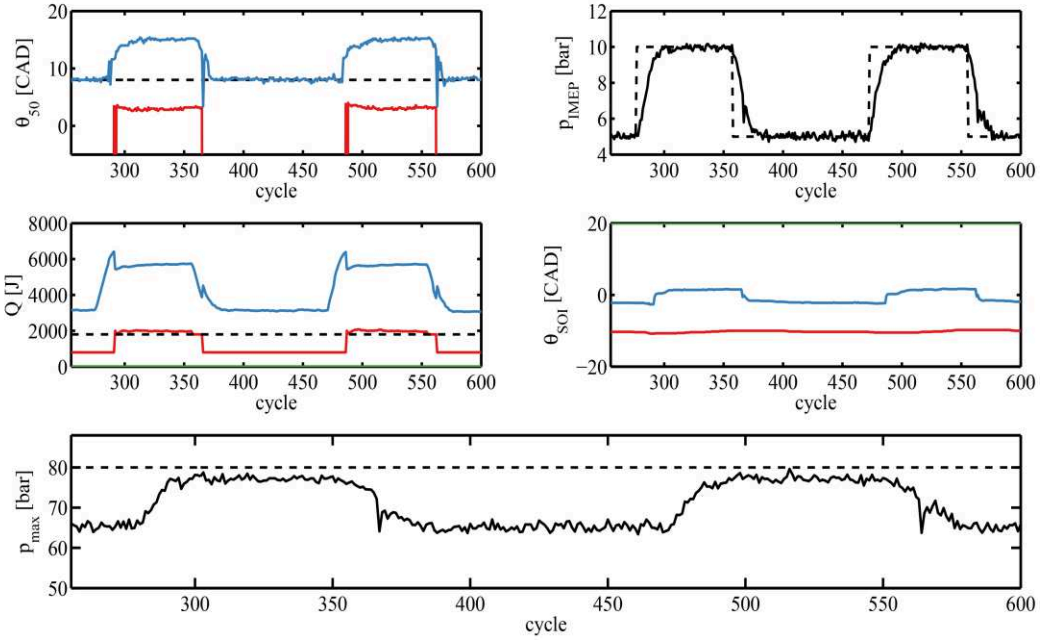

Figure 25 p_{max}-constraint evaluation. The controller was set to follow p_{IMEP} step changes from 5 to 10 bar. Increasing p_{IMEP} to 10 bar with a single injection and maintained θ_{SOI} violates $c_{p_{max}} = 80\ bar$. The controller acts by increasing m_f^1 as the constraint is approached.This results in an additional detected combustion timing after TDC, moreover θ_{SOI} is delayed 8 crank-angle degrees for constraint fulfillment.

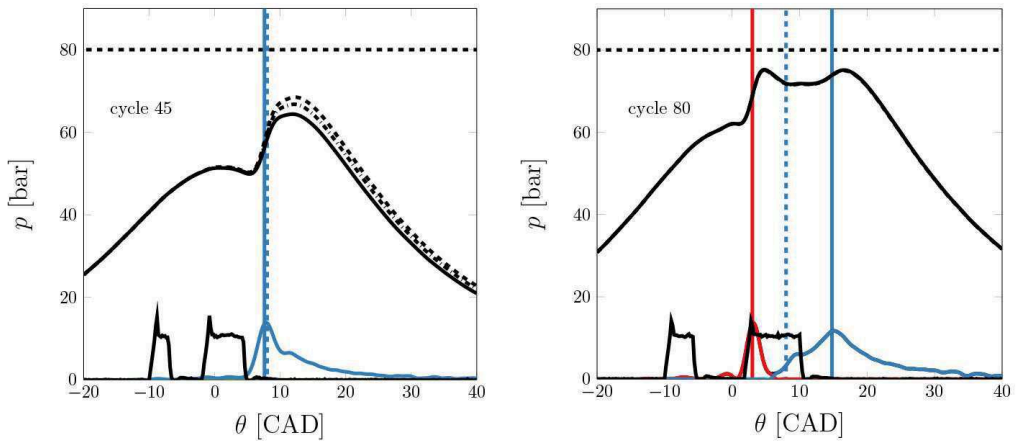

Figure 26 In-cycle data for cycle 45 (left) and 80 (right) from Fig. 3. In-cylinder pressure, injector current and $dQ_c/d\theta$ are presented together with the vertical lines indicating θ_{CT} and θ_{CT}^{ref}. The dashed pressure curves visible at cycle 45 are predicted cylinder pressure for two subsequent engine cycles. The increase in predicted cylinder pressure is due to the increase in p_{IMEP}^{ref}. Two θ_{CT} are detected at cycle 80 due to the increase in m_f^1 and θ_{SOI}^2.

The controller with optimziation problem 2 above was evaluated by varying the reference pressure trajectory, p_{ref}. The controller's ability to follow pressure reference changes with two injections is presented in Figure 26. In this experiment the constant volume to constant pressure ratio of the pressure reference curve (dashed) changes from 0.5 (red) to (blue) 0.2. The different pressure curves (solid) are consecutive engine cycles during the transition from p_{ref}^1 (red) to p_{ref}^2 (blue).

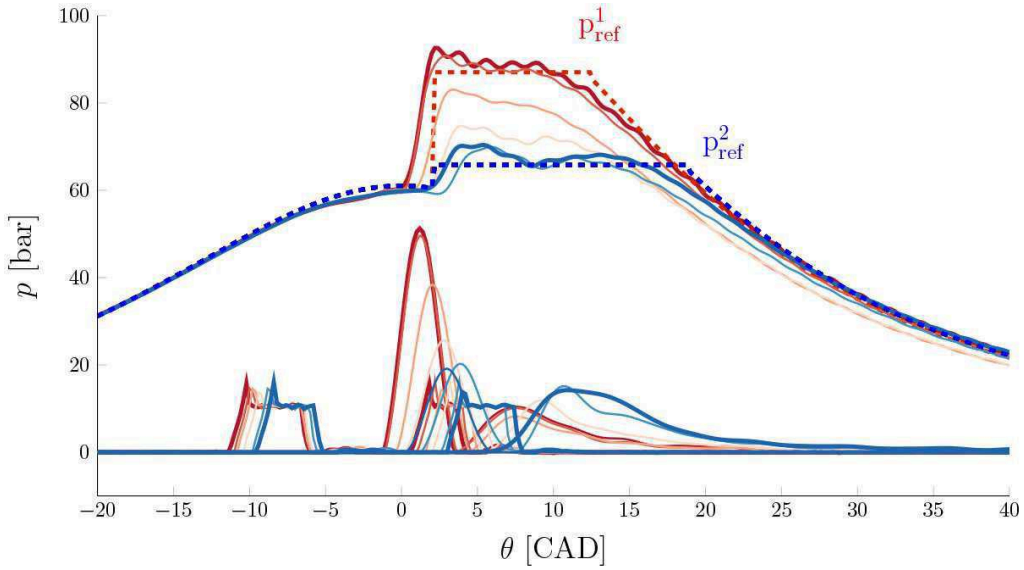

Figure 27 The controller's ability to follow pressure reference changes with two injections. In this experiment the constant volume to constant pressure ratio of the pressure reference curve (dashed) changes from 0.5 (red) to (blue) 0.2.

Summary and Conclusions

Two model predictive controllers were presented and experimentally evaluated. Both controllers utilized first principles physical models in order to locally predict in-cylinder pressure changes due to fuel-injection changes. Experimental results obtained from the Scania D13 heavy-duty engine showed

- Fulfillment constraints on pressure, pressure-rise rate, engine-out NO emissions and exhaust temperature during load changes.
- Tracking of in-cylinder limited-pressure reference trajectories.

The presented above results will be published during 2018.

Publications during 2017

Ingesson, Gabriel, et al. "Efficiency optimal, maximum-pressure control in compression-ignition engines." American Control Conference (ACC), 2017. IEEE, 2017.

Ingesson, Gabriel, et al. "An investigation on ignition-delay modelling for control." International Journal of Powertrains 6.3 (2017): 282-306.

References

Ingesson, G., L. Yin, R. Johansson, and P. Tunestål (2015): A Model-Based Injection-Timing Strategy for Combustion-Timing Control," SAE Int.J. of Engines, 8, 1012-1020.

Muric, K., O. Stenlåås, and P. Tunestål (2014): Zero-dimensional modeling of NOx formation with least squares interpolation," Int. J. of Engine Research, 15, 944-953.

Eriksson, L. and L. Nielsen (2014): Modeling and control of engines and drivelines, Chichester, West Sussex, United Kingdom: John Wiley & Sons.

Gas path control

Introduction

This project focuses on Partially Premixed Combustion (PPC) multi-cylinder engine control. The purpose is to develop advanced control oriented model and control algorithm to optimize the engine efficiency and maintain low engine emission at the same time. The effort was taken both on gas exchange system and combustion process control. In the last year, some part of work was done to investigate the gas system control for PPC engine; a nonlinear control method was investigated to control the gas system. A preliminary control structure is also developed for transient control.

Control Structure

The proposed preliminary control structure enabling simple transient control of a PPC multi-cylinder engine is illustrated in Figure 28. Based on required engine load and speed, the reference model generates corresponding references of combustion timing, inlet pressure, EGR flow rate and so on. The engine load gets feedback from IMEP using cylinder pressure sensor, so is the combustion timing. The air path used feedback signal of inlet pressure and estimated EGR from to control the EGR and VGT valves achieving target values. The detail model and control structures can be found in later section

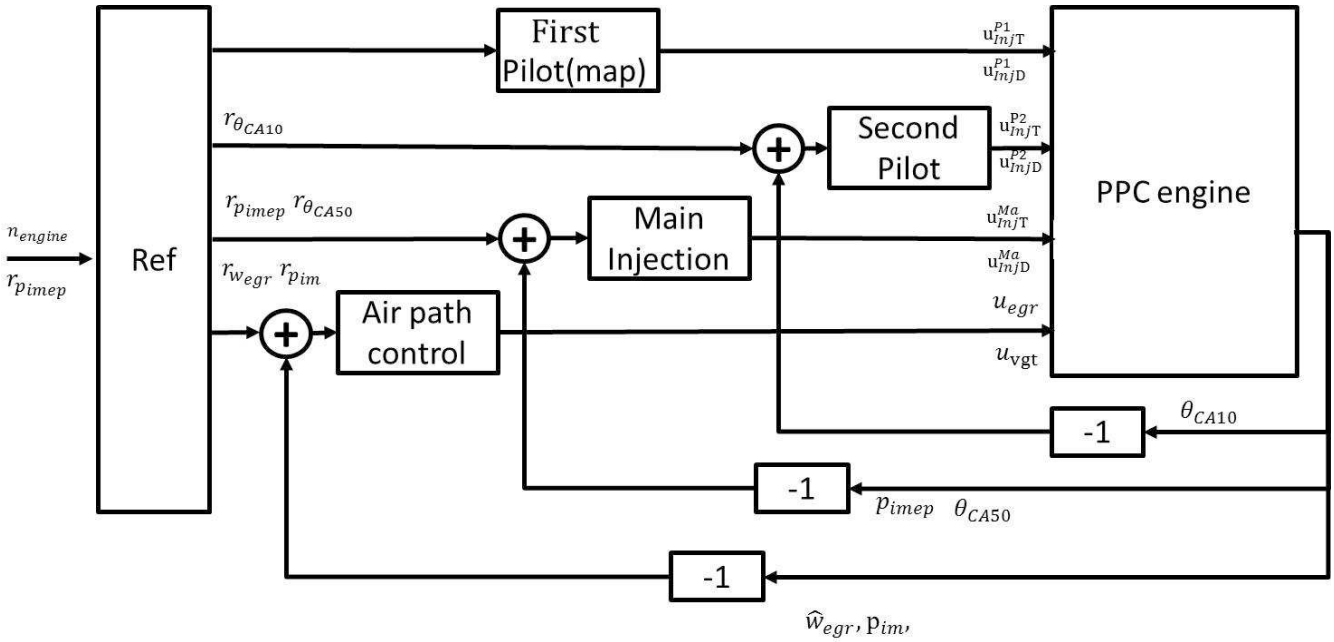

Figure 28. General control structure

The combustion modeling and control

The models of combustion duration and ignition delay validation are plotted in in Figure 29 and Figure 30. The model is used in MPC structure to control the combustion timing and also prevent early ignition at the same time.

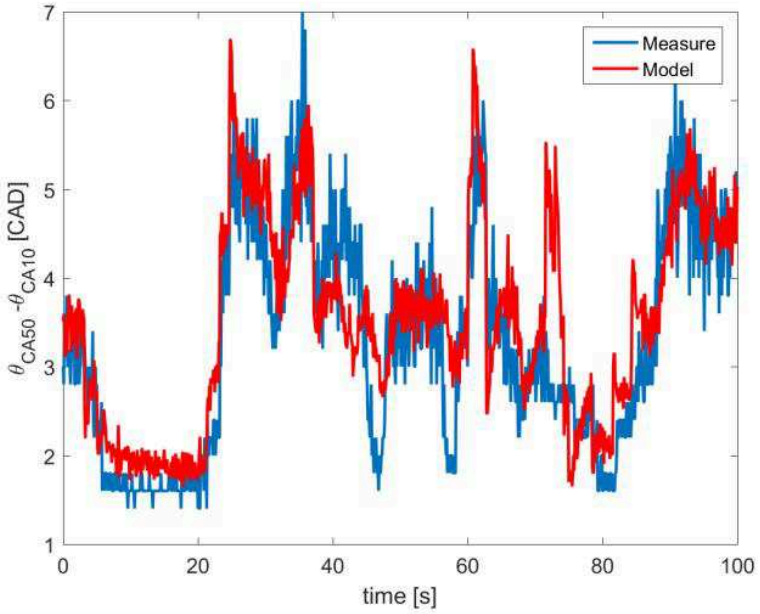

Figure 29. Combustion duration

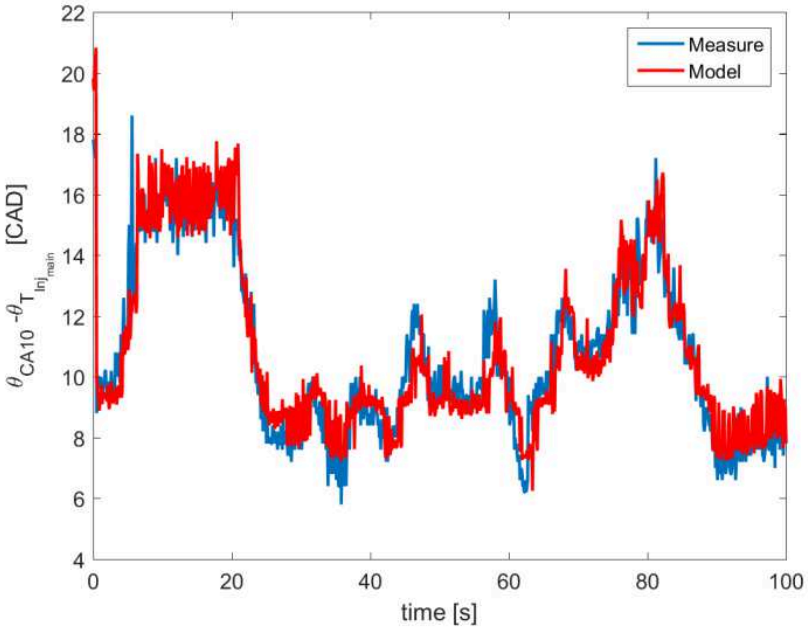

Figure 30. Ignition delay

The nonlinear controller for gas-path control

A new framework for gas-path control with VGT and EGR was investigated. The idea is to develop the sliding mode control in a receding horizon way, the propose controller was tested on gas-path control and compared with a model predictive controller, results are shown in Figure 32.

Transient control results

The general control method of MPC coupled with extended state estimator (Kalman filter) formed the general feedback structure of the controller (Figure 31) are used in both combustion timing and air path control.

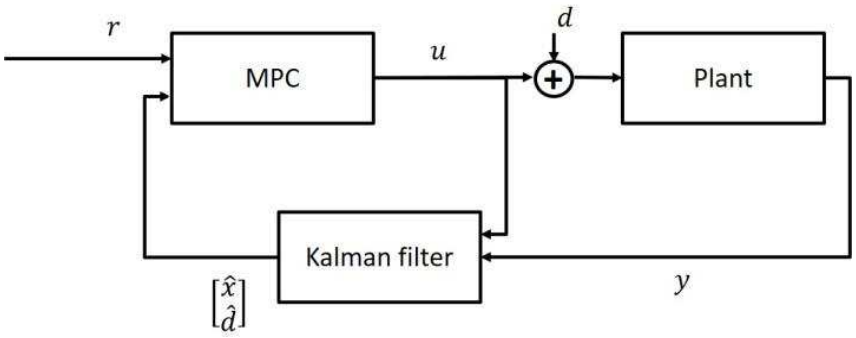

Figure 31. MPC structure

The transient scenarios are simple load step responses from low to high load, the results are shown in Figure 33. In general, the combustion timing, inlet pressure and EGR flow followed the references. There are some overshoots in the IMEP, which resulted from the feedforwards terms. And the overshoots in IMEP also resulted in the combustion timing overshoots.

Future work

The future work remains on the efficiency optimization by optimizing the in-cylinder stratification and reducing the heat transfer losses.

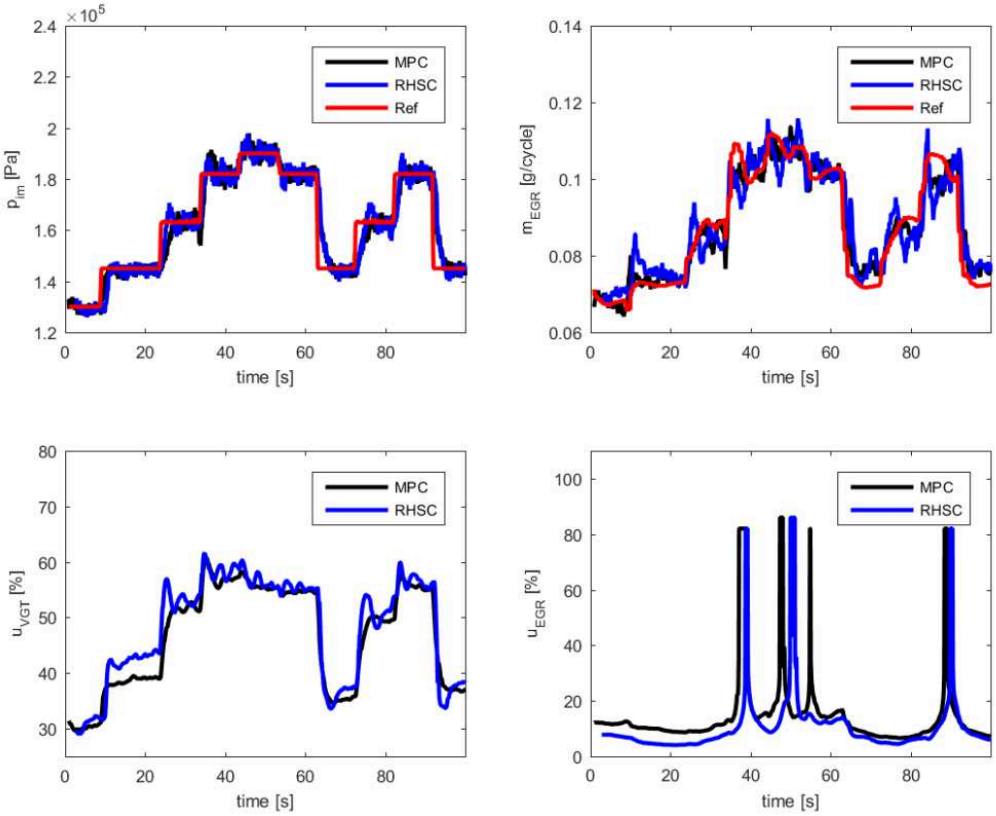

Figure 32. Comparison of receding horizon sliding controller and model predictive controller.

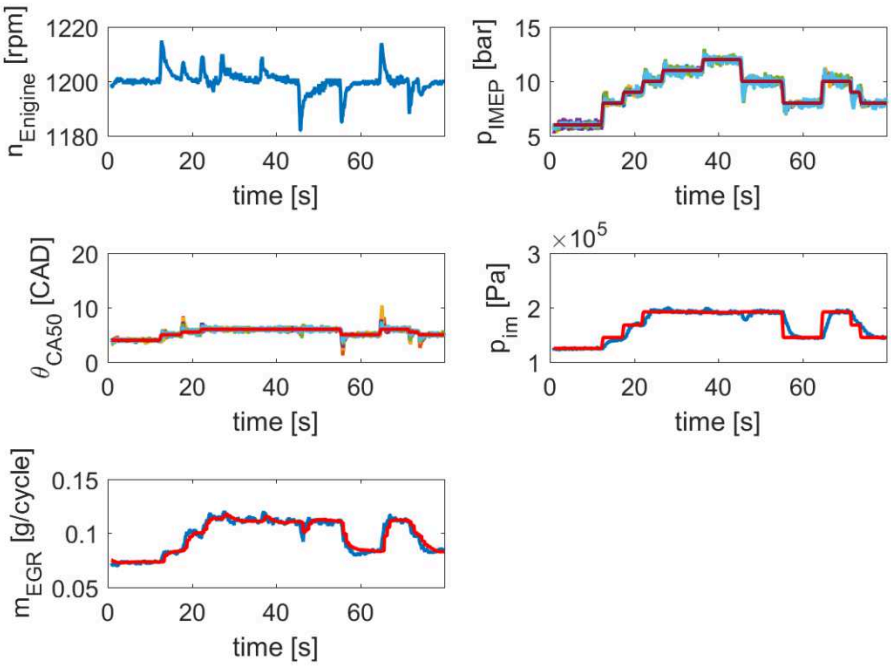

Figure 33. Transient control results

GenDies Project

The GenDies project studies processes in Diesel engines that are of general interest to the Diesel engine community. During the 2014-2017 program period the focus has been on optical studies of soot formation and oxidation.

Ted Lind
PhD Student

Post injection mechanisms elucidated by the use of diffused back-illumination soot extinction imaging.

Small closely-coupled post injections of fuel in diesel engines are known to reduce engine-out soot emissions, but the relative roles of various underlying in-cylinder mechanisms have not been established. Furthermore, the efficacy of soot reduction is not universal, and depends in unclear ways on operating conditions and injection schedule, among other factors. To gain more insight into in-cylinder processes affecting soot with post-injections, diffused back-illumination imaging (DBI) technique is utilized. The DBI setup developed for this experiment enables quantitative 2-dimensional (2D) line-of-sight optical thickness (KL) measurements from soot extinction with a temporal resolution of 42 kHz. The high temporal resolution and relatively large field of view (FoV) quantifies the evolution of in-cylinder soot for roughly the downstream half of one diesel jet of the multi-hole injector throughout each cycle.

A common way of estimating the amount of in-cylinder soot is through the use of natural luminosity (NL) imaging. DBI imaging shows that there is a very poor correlation between the amount of natural luminosity and the amount of soot. This can be seen in Figure 34 where the normalized NL is compared to the normalized KL values obtained from the DBI imaging.

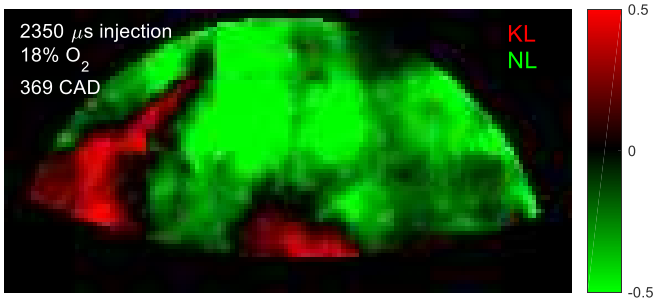

Figure 34 False color comparison between NL and KL within the DBI FoV

The DBI imaging also reveals that, when the post injection is sufficiently short, the majority of the soot in the post injection is oxidized even before the post injection reaches the piston bowl wall, thus allowing for increased load with similar soot emissions compared to a single-injection condition. However, for longer post injections the plenty of soot is left un-oxidized. This is shown in Figure 35a where the average KL within the FoV is shown. The 400 µs post injection case is all but indistinguishable from the 2350 µs single injection case suggesting that all the soot formed in the post injection is quickly oxidized. For the 800 µs post injection the results are vastly different. Here it is clear that plenty of soot from the post reaches the FoV and is left oxidized by the end of the cycle leading to a situation where the post injection strategy creates more soot emissions than a load equivalent single injection strategy as seen in Figure 35b.

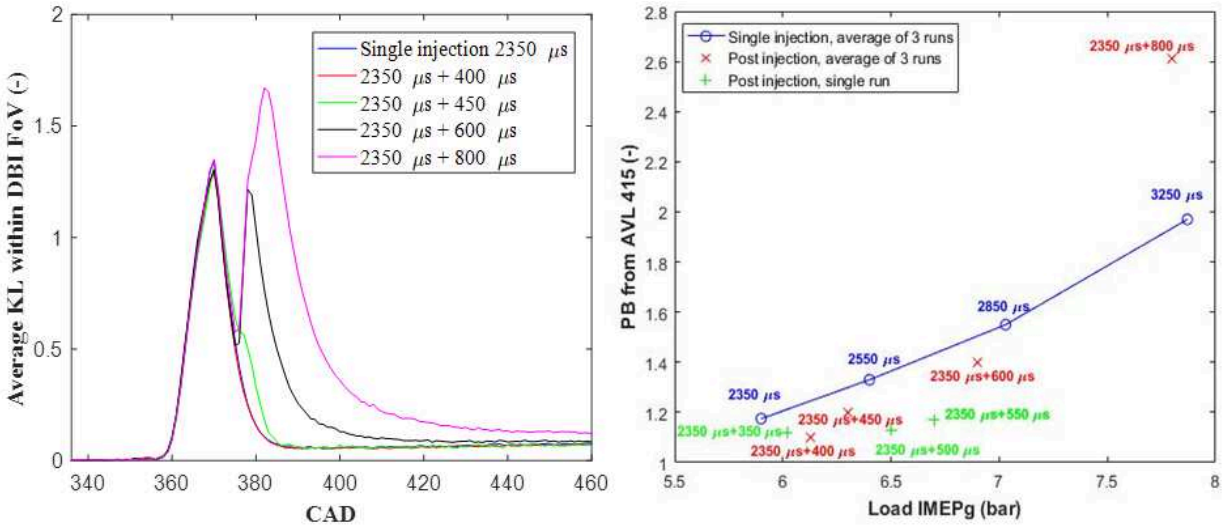

Figure 35 a, Evolution of KL within the DBI FoV for several post injection strategies and a single injection strategy 2b Soot vs load plot of various post and single injection strategies as 18 % O_2

A transient increase in entrainment that occurs after the end of injection (the "entrainment wave") is a candidate explanation for the observed completeness of post-injection soot oxidation. Additionally, semi-quantitative comparisons of soot KL and natural luminosity trends seen in Figure 36 a&b reveal decreasing KL accompanied by increasing NL. This observation is consistent with an increase in post-injection soot temperature after the end of the post injection, which may further aid oxidation.

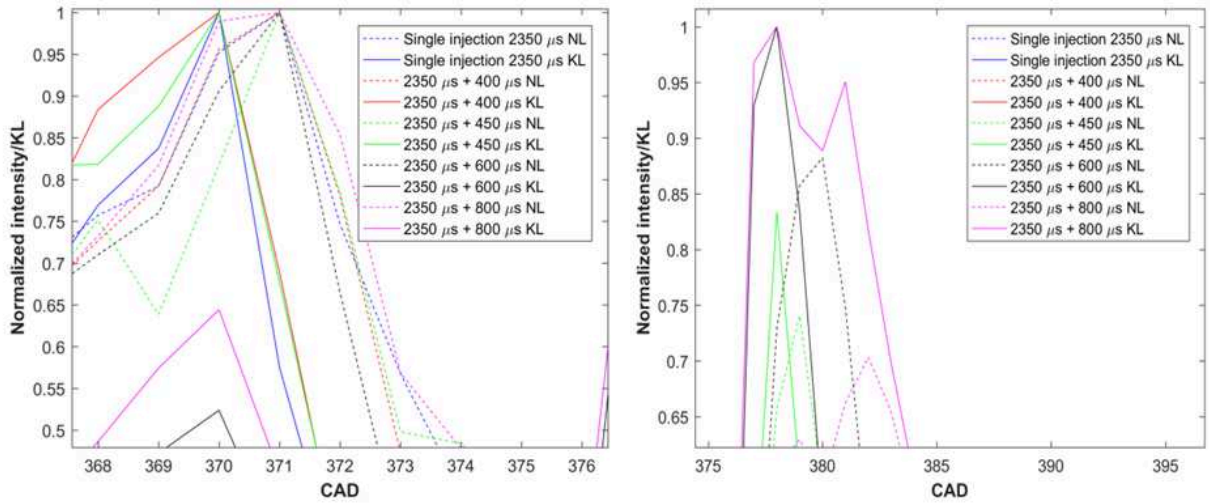

Figure 36 a & b Normalized KL and NL values for several post injection strategies revealing that the highest luminosity always occur after the peak KL value.

Michael Denny
PhD Student

Mechanisms of pilot and post injection strategies in a LD, optical diesel engine.

Background

Due to customer expectations on perceived engine noise and tightening emissions regulations, pilot injections—small quantities of fuel injected before the main injection—are commonplace to mitigate both noise and NO_x emissions. Post injections are also implemented in order to reduce the engine-out soot emissions.

Fuel injection equipment technology has advanced over the years by increasing operating pressures, shortening dwell times between injections, and reducing the minimum injected mass per injection event. This has led to a change in injection strategies which allow for an improvement in efficiency and combustion noise. Understanding the mechanisms occurring in-cylinder with these new injection strategies is the main goal of this project.

Current Results

The most recent work studies differences in engine performance attributes when changing injection strategies. A double-pilot injection strategy with a modest dwell time between injections is compared to two different triple-pilot injection strategies with significantly reduced dwell times.

These later strategies are referred to as being closely-coupled, as a result of their short dwell time. Beyond the aforementioned benefits in increased efficiency and decreased combustion noise, several further conclusions are drawn from the study. The combustion noise reduction is due to a decrease in the undulation of the pressure trace. This reduction is the result of a reduced undulation in the heat release rate within the same spectral range as that attributed to the strongest contributing frequencies for combustion noise in the pressure trace.

A new metric is developed to quantify changes in the heat release rate and whether or not they are likely to lead to decreased combustion noise. This metric is called the ratio of reduced heat release and it indicates how close or far a heat release is to being linear. For the injection strategies studied, reducing the ratio of reduced heat release lead to a reduced combustion noise. This confirmed the hypothesis that the undulation in the heat release rate is responsible for the combustion noise produced from the cycle.

The results from this study in the metal engine laid down the understanding and need for further investigation into the combustion development processes of these more advanced triple-pilot injection strategies. The second study, which was completed during 2017, builds upon the first by investigating these same strategies via high speed video (HSV) recordings of the combustion processes in the geometrically similar optical engine. Significant rework was performed to obtain better optical data compared to the prior results from earlier in the year. Analysis of this experiment is currently underway.

Figure 37 shows preliminary but detailed HSV images both very early in the cycle (before combustion) and late in the cycle (at the end of the main injection).

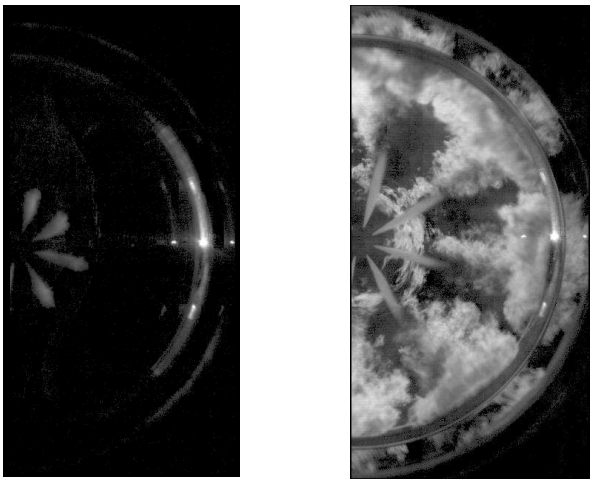

Figure 37: Preliminary HSV images of 1 crank angle degree of combustion development (left to right) during the beginning of the main injection's heat release for the reference case (top) and strategy B (bottom).

Gas Engine Project

The Gas Engine Project studies phenomena that are of importance for the efficiency and emissions of gaseous-fuelled engines with focus on methane-based fuels. In the 2014-2017 program period the focus has been on prechamber technologies and dual-fuel technologies as means for increased efficiency through lean operation.

Saeed Derafshzan
PhD Student

Pablo Garcia
PhD Student

Introduction

The Gas Engine Project aims to explore and understand the combustion phenomenon in engines operating on gaseous fuels and develop technologies as an alternative to present day diesel operated combustion engines which are facing severe challenges like stringent emissions norms, high technology cost and unsustainable fuel supply. Currently, the focus is pilot-ignited natural gas diesel dual fuel combustion. Even though this concept has been already commercialized and different solutions exist in industry, the fundamental mechanism of ignition and interaction between diesel and natural gas remains unclear. For this reason, this new phase aims for understanding and gaining deeper insight into this mechanism using single-cylinder metal and optical studies.

Background

Recent emissions legislation in the marine sector has emphasized the need to reduce NO_X as well as sulphur emissions. The fulfilment of these limits with conventional marine diesel oil requires expensive aftertreatment systems. Apart, the development of fossil-free energy sources, such as wind power or solar energy, has introduced the need for back-up energy sources which can compensate for quick variations in energy demand in an efficient way. In this context, pilot-ignited dual fuel internal combustion engines have emerged as an efficient and clear solution both for marine and power sectors.

During this dual fuel mode, diesel fuel is used as the source of ignition of the port injected natural gas. Traditionally, diesel fuel is injected close to top dead center, when thermodynamic conditions in the combustion chamber turn out in short ignition delay and, consequently, in stable combustion. However, high in-cylinder local temperature and pressure enhances NO_X formation and the risk of knocking cycles. For these reasons, large-bore dual fuel marine engines are operated using early diesel pilot injection timings, which result in longer ignition delay and consequently more diesel fuel premixing prior to self-ignition. However, excessively long ignition delay causes poor ignition quality and therefore combustion stability problems. This temperature trade-off between low enough temperature for controlling NO_X levels/knock probability but high enough for sustained diesel autoignition severely limits the operating region of large bore medium speed dual fuel engines. This proves the importance of understanding properly the behavior of the diesel pilot injection in natural gas mixtures.

Project Overview

- *Phase 1: Metal Engine Experiments*

This stage was mainly focused on screening diesel pilot injection behavior under different diesel ignition delay conditions. The goal was to define the overall characteristics of the combustion process and understand, via 1-D simulations of diesel spray pattern, the influence of diesel dilution on the ignition process. This simulation work was performed in collaboration with Dr. Antonio Garcia, from CMT-Motores Térmicos (Spain). This stage ended by March 2017 with the following journal publication:

P. García-Valladolid, P. Tunestal, J. Monsalve-Serrano, A. García, J. Hyvönen. *Impact of diesel pilot distribution on the ignition process of a dual fuel medium speed marine engine.* Energy Conversion Management, 149 (1) (Oct 2017), pp. 192-205

- *Phase 2: Optical Engine Experiments*

Figure 38: Wärtsilä 20 DF optical engine equipped with variable valve actuation.

This phase started in March 2017 with the conversion of the 20cm bore single cylinder metal engine to optical configuration. It consists of a Bowditch design with optical access through piston and side-windows (Figure 38). The goal is to firstly generate a conceptual model of the ignition process in pilot-ignited dual fuel combustion and, later, focus into a deeper understanding of the fundamental properties that affect the autoignition of the pilot fuel in a natural gas lean mixture environment.

Methods

Firstly, chemiluminescence was recorded with high-speed camera for visualization of the ignition process and initialization of the combustion process. Using high speed CMOS camera (Photron FASTCAM SA-Z) and appropriate filters to suppress soot luminosity, 0.2 CAD resolved chemiluminescence can be visualized (800rpm, skip-fire engine operation). In a later stage, laser-based techniques will be applied for pilot fuel tracing.

Recent Progress

The optical engine was fired on July 2017 for the first time. Unfortunately, the progress of this project at this stage has been limited by technical problems which have appeared during the testing of this novel optical engine. The main limitation was due to excessive amount of oil scraping from the lower piston and causing wetting of the optical mirror and optical piston base. Different solutions have been tested although no optimal solution has been found yet. The use of vacuum generators (both around mirror and in crankcase), the reduction of lower piston oil cooling flow, the use of flanges around

piston extension as barriers for droplets, alternative piston ring rack, etc. have been tested. At the same time, attempts to capture images with better signal intensity from lean mixtures have been carried out. Using appropriate filters for eliminating soot luminosity and utilizing lenses with different properties, along with the progress in eliminating the excessive oil from the piston and mirror, the quality of the images was improved. However, in December 2017, a piston seizure caused further delay. Lund technical team and Wärtsilä are currently working on these issues.

Future Work

Engine experiments performed in Phase 1 provided good insight into the characteristics of the ignition process, but the fundamental mechanism of ignition in the main chamber remains unclear. Phase 1 ended in February 2017. Optical techniques to be applied in Phase 2 will reinforce this area and provide more fundamental data with higher value for the research community. Phase 2 started in March 2017. The lower piston oil cooling system is currently under redesign and it will be tested during the first half of 2018. Initially, high speed video imaging of the combustion process will be performed, followed by pilot fuel tracing at a later stage.